TRANS **NOW**

TRANSPORTATION NORTHWEST

Final Report TNW2012-16

Research Project Agreement No. 62-0943

Simulation-Based Testbed Development for Analyzing Toll Impacts on Freeway Travel

by

Yinhai Wang	Yunteng Lao	Cathy Liu	Guangning Xu
Professor	Graduate Research Assistant	Graduate Research Assistant	Visiting Graduate Student

Department of Civil and Environmental Engineering
University of Washington
Seattle, Washington, 98195-2700

Sponsored by

Transportation Northwest (TransNow)
University of Washington
135 More Hall, Box 352700
Seattle, Washington 98195-2700

Washington State Department of Transportation (WSDOT)
310 Maple Park Avenue SE
PO Box 47300
Olympia, WA 98504-7300

and in cooperation with

U.S. Department of Transportation
Federal Highway Administration

A

Report prepared for:
Transportation Northwest (TransNow)
Department of Civil and Environmental Engineering
129 More Hall
University of Washington, Box 352700
Seattle, Washington 98195-2700

June 2012

TECHNICAL REPORT STANDARD TITLE PAGE

1. REPORT NO.	2. GOVERNMENT ACCESSION NO.	3. RECIPIENT'S CATALOG NO.
TNW 2012-16		

4. TITLE AND SUBTITLE	5. REPORT DATE
Simulation-Based Testbed Development for Analyzing Toll Impacts on Freeway Travel	June 2012
	6. PERFORMING ORGANIZATION CODE
7. AUTHOR(S)	8. PERFORMING ORGANIZATION REPORT NO.
Yinhai Wang, Yunteng Lao, Cathy Liu, and Guangning Xu	TNW2012-16
9. PERFORMING ORGANIZATION NAME AND ADDRESS	10. WORK UNIT NO.
Transportation Northwest Regional Center X (TransNow) Box 352700, 123 More Hall University of Washington Seattle, WA 98195-2700	11. CONTRACT OR GRANT NO. DTRT07-G-0010
12. SPONSORING AGENCY NAME AND ADDRESS	13. TYPE OF REPORT AND PERIOD COVERED Final Report
	14. SPONSORING AGENCY CODE

15. SUPPLEMENTARY NOTES

This study was conducted in cooperation with University of Washington and the U.S. Department of Transportation

16. ABSTRACT

Traffic congestion has been a world-wide problem in metropolitan areas all over the world. Toll-based traffic management is one of the most applicable solutions against freeway congestion. This research chooses two toll roads, the SR-167 HOT Lane and the SR-520 toll Bridge (i.e. Evergreen Point Bridge), as study sites for simulation testbed developments to evaluate the toll impact on freeway operations.

The research approach proposed in this study consists of three steps: first, external modules are developed to enable VISSIM models to simulate various traffic operations with complicated tolling schemes; then, a standardized calibration procedure is proposed for freeway traffic simulation to enhance the models' creditability; and finally, a statistical method is developed to analyze simulation outputs against data autocorrelation problems.

Two VISSIM external modules were developed for evaluating toll impacts on freeway operations in this research. For the SR-167 HOT Lane site, an external tolling control module using the Component Object Model (COM) interfaces was developed to dynamically adjust the toll rate based on real time traffic conditions. For the SR-520 Evergreen Point Bridge site, an external routing module using Car2X module is developed to dynamically update vehicle routing. These external modules enabled testing customized tolling strategies often needed in toll impact studies.

The simulation results from the SR-167 HOT Lane study site found that among all the three operational strategies, HOT Lane Operation with Dynamic Toll outperforms the other two strategies under various traffic demand conditions. Compared with the HOV Lane Operation, Dynamic Toll strategy makes significant improvement on GP lane performance at regular segments, merging areas, on-ramps, and off-ramps. Compared with the Time-of-day Toll Rate strategy, Dynamic Toll strategy is more flexible under a variety of traffic demands. The simulation results of the SR-520 toll Bridge found that with an increase in toll at SR-520, the travel speed on SR-520 tends to increase and the speed on I-90 tends to decrease as more vehicles are diverted to use the non-tolled alternative. However, the change on I-5 and I-405 after tolling is insignificant since the number of vehicles turning from SR-520 to I-90 is much smaller than the existing volumes on I-5 and I-405.

The two simulation testbeds developed in this study were applied to the SR-520 Evergreen Point Bridge and the SR-167 HOT Lane projects and the results were satisfactory. These testbeds are capable of studying various customized tolling strategies on freeway operations. The methodology developed in this study for external module development and simulation output analysis can be used to other simulation studies of similar kinds.

17. KEY WORDS	18. DISTRIBUTION STATEMENT
Congestion pricing, Tolling, Simulation	No restrictions. This document is available to the public through the National Technical Information Service, Springfield, VA 22616

19. SECURITY CLASSIF. (of this report)	20. SECURITY CLASSIF. (of this page)	21. NO. OF PAGES	22. PRICE
None	None		

DISCLAIMER

The contents of this report reflect the views of the authors, who are responsible for the facts and accuracy of the data presented herein. This document is disseminated through the Transportation Northwest (TransNow) Regional Center under the sponsorship of the U.S. Department of Transportation UTC Grant Program. The U.S. Government assumes no liability for the contents or use thereof. Sponsorship for the local match portion of this research project was provided by the Washington State Department of Transportation. The contents do not necessarily reflect the views or policies of the U.S. Department of Transportation or Washington State Department of Transportation. This report does not constitute a standard, specification, or regulation.

CONTENTS

LIST OF FIGURES

LIST OF TABLES

EXECUTIVE SUMMARY

Traffic congestion costs billions of dollars every year, including lost time, excess fuel consumption, air pollution, and lost productivity. Constructing more roadways has been a traditional solution to solving traffic congestion problems. However, due to the high cost, long construction cycle, and complicated procedure for building new transportation infrastructures, the increase in roadway supply was lagged far behind the increase in demand.

An alternative solution to address this issue is to manage the existing infrastructure more efficiently with advanced traffic control and management technologies in addition to travel demand control. Based on previous studies, toll-based traffic management is one of the most applicable solutions against freeway congestion. This leads to this study on the tolling impact on traffic network performance.

Since the tolling strategy may differ from time to time and from location to location, simulation-based evaluation is of practical importance for traffic engineers to quantify toll impacts, optimize tolling strategies, and identify potential problems prior to the implementation of different scenarios. This research chose two toll roads as study sites to evaluate the toll impact on freeway. Simulation testbeds were developed for these study sites, the High Occupancy Toll (HOT) lane on SR 167 and the SR-520 toll Bridge, using the VISSIM microscopic simulation package for investigation alternative tolling and management strategies.

Although VISSIM is widely utilized for freeway modeling, it cannot handle vehicle routing issues resulted from dynamic tolling strategies with its built-in modules. Review of previous studies did not find any published materials describing VISSIM-based traffic simulation with dynamic tolling schemes. Therefore, further research effort for enabling VISSIM models to simulate traffic operations under dynamic tolling strategies is highly desired.

The research approach proposed in this study consists of three steps: first, external modules are developed to enable VISSIM models to simulate various traffic operations with complicated tolling schemes; then, a standardized calibration procedure is proposed for freeway traffic simulation to enhance the models' creditability; and finally, a statistical method is developed to analyze simulation outputs against data autocorrelation problems.

Specifically, two VISSIM external modules were developed in this research. For the SR-167 HOT simulation, an external tolling control module using the Component Object Model (COM) interface was developed to dynamically adjust the toll rate based on real time traffic conditions.

For the SR-520 toll Bridge simulation, an external routing module using the Car2X function was developed to dynamically update vehicle routing.

For the SR-167 HOT simulation, three operational strategies (High Occupancy Vehicle (HOV) Lane Operations, Time-of-Day Toll Operations, and HOT Lane with Dynamic Toll Operations) and three traffic demand conditions were considered and implemented in this research. Our simulation experiments resulted in the following findings:

- Among all the three operational strategies, HOT Lane Operation with Dynamic Toll (Strategy III) outperforms the other two strategies under all three traffic demand conditions.
- Comparing with the HOV Lane Operation (Strategy I), Strategy III makes significant improvement on General Purpose (GP) lane performance. The performance enhancement on the overall freeway (GP+HOV/HOT), merging areas, on-ramps, and off-ramps are evident as well. For example, the improvement on the speed of the overall freeway ranges from 10% to 80% for this study site.
- Comparing with the Time-of-day Toll Rate (Strategy II), the overall network performance under Strategy III is also better under a variety of traffic demands. It further proves that Strategy III is more responsive to different traffic conditions.
- Comparing with the other two strategies, Strategy III also reduces the emission and network delays as well.

For the SR-520 toll bridge simulation, two scenarios were considered. In Scenario 1, in order to identify the tolling impact, the traffic demand is assumed to be the same before and after the toll implementation. Four different toll rates were considered in this scenario: $0, $1, $3.5, $7. In Scenario 2, it is assumed that after the tolling implementation, there is a 5% reduction in the traffic demand crossing the Lake Washington during peak hour. This assumption is reasonable since during the peak hour with a higher travel cost some travelers tend to switch their travel to other time period or modes or other destinations. The simulation results for the SR 520 Bridge identified the following facts:

- With an increase in toll at SR-520, the total throughput on SR-520 tends to decrease and the throughput on I-90 tends to increase as more vehicles are diverted to use the non-tolled alternative. However, the throughput on I-90 did not increase significantly since the traffic demand on I-90 is already at or close to the capacity during the peak hours.

- The impact on I-5 and I-405 is not quite pronounced since the throughput shift from SR-520 to I-90 and I-405 is relative small compare to their capacity.
- The impact on the speed and volume on the network from the simulation under scenario 2 is similar to the loop data collected from the peak hour after tolling.

Based on the findings of the simulation results and the observed traffic phenomena, the research team would like to make the following recommendations:

- Use dynamic tolling strategy when possible since it is more flexible to respond to the real-time traffic conditions than other tolling strategies.
- More research is desired for improving the accessibility from I-450 to I-90 and from SR-520 WB to I-405 SB when SR-520 is tolled.
- More research is needed for developing traffic responsive dynamic tolling strategies.

CHAPTER 1 INTRODUCTION

1.1 Research Background

From 1980 to 2009, yearly Vehicle Miles Traveled (VMT) increased by 95%, while road mileage increased by only about 4.9% nationwide (Bureau of Transportation Statistics, 2010). The enlarging gap between the increasing travel demand and limited infrastructure expansion has worsened the traffic congestion, especially in the metropolitan areas. Traffic congestion costs billions of dollars each year, including lost time, excess fuel consumption, air pollution, and lost productivity. The Texas Transportation Institute (TTI) conducts an annual survey of traffic congestion in US urban areas. According to the 2011 Urban Mobility Report (Shrank and Lomax, 2011), annual delay per person was 34.4 hours in the 439 U.S. urban areas in 2010, a 139% increase compared to that in 1982. Congestion cost an average of $713 per traveler in the surveyed urban areas in 2010. In the Greater Seattle area, traffic congestion resulted in a total of 87.92 million hours of travel delay and 46.37 million gallons of excess fuel consumption in 2010, which corresponded to a congestion cost of 1.91 billion dollars, ranking the 12th highest in the U.S. (Shrank and Lomax 2010). Constructing more roadways has been a traditional solution to solving traffic congestion problems. However, due to high cost, long construction cycle, and complicated procedure for building new transportation infrastructures, the increase in roadway supply was lagged far behind the increase in demand. An alternative solution to address this issue is to manage the existing infrastructure more efficiently with advanced traffic control and management technologies in addition to travel demand control, like speed harmonization and ramp metering control.

Of these technology solutions, toll-based traffic management has been regarded as one of the most applicable countermeasures against freeway congestion. Since the first toll road was built to connect Philadelphia and Lancaster in 1795, it has been a long tradition for toll traffic facilities in the U.S. (Encyclopedia Britannica, 2005). For congested freeway corridors, charging a toll to the users can help allocate traffic demand more efficiently, and therefore, better utilize the facility and reduce congestion. Besides its capability of optimizing the resource allocation, it proofs that toll-based traffic management can provide better infrastructure maintenance and generate funds for road construction and capacity improvements through tolling collection (CBO, 1997). Currently, there are more than 300 tolled facilities in operation in the U.S. (Holguin-Veras, et al. 2006). These facilities are sporadically distributed in various operational conditions, from super-congested corridors in large metropolitan areas to rural highways. Typical toll payment formats in the U.S. include manual toll collection and electronic toll collection. The tolling mechanisms are diversified from multi-tier toll structures corresponding to different commuter types, time of day, traffic condition, and such, to simple toll settings that are only based on the number of axles per vehicle.

Over the past decade, HOT lane has been proposed as another representative toll-based traffic management technology. This concept has originated from the High Occupancy Vehicle (HOV) lane, which aims at motivating people to shift from Single Occupancy Vehicles (SOV) to carpools or buses in order to reduce SOV trips and traffic congestion (Kim et al, 2002). However, studies on the usage of HOV lanes indicated many HOV facilities are underutilized in certain time periods when the adjacent General Purpose (GP) lanes are congested (Dahlgren, 1998, and Kwon and Varaiya 2005). Therefore, converting HOV lanes to HOT lanes can create a win-win solution to reduce traffic delays and enhance total traffic throughputs. SOVs are allowed to pay a toll for using HOV lanes and the excess capacities of HOV lanes can be better utilized. Currently, there are more than 1,300 miles of HOV lanes in the U.S. (Chu, et al. 2007). Successful operation of HOT lanes by fully exploiting their excess capacities can potentially generate huge time savings and significantly mitigate traffic congestion. The first HOT lane project was implemented on State Route 91 in Orange County, California in 1995. After that, three other states: Texas, Minnesota, and Colorado also implemented HOT lanes (Myron, and Ungemah, 2006). In practice, dynamic pricing strategies have been implemented. Many studies (Appiah et al., 2005, Halvorson, et al., 2006, Yin and Lou, 2007, Zmud, et al. 2007, Zhang, et al., 2008, Zhang, et al., 2009, and Mowday, 2006) were conducted to investigate optimal tolling strategies and evaluate the HOT lane system performance. For example, the basic price varies from \$0.50 to \$4.00 according to time of day for the I-15 HOT lane in San Diego. The tolls can be adjusted in response to real-time traffic conditions. For the I-394 MnPass Express lane in Minnesota, a similar pricing mechanism is implemented. The tolls are adjusted upward or downward to ensure the HOT lane speed is around 50-55 mph. The toll rate is updated every three minutes. The toll rate for I-394 MnPass Express lane ranges from 25 cents to \$8 (Zmud, et al., 2007).

These theoretical studies and practical experience on toll-based traffic management provide valuable insights for in-depth understanding of toll impacts and tolling optimization in the network. However, toll-based traffic operations are closely associated with many location-specific factors, such as local economic conditions, traffic compositions, travel patterns, geographic characteristics, and population distribution, etc. The previous knowledge and investigations may not be directly applicable to accommodate various situations of new toll traffic projects due to heterogeneous users, diverse travel patterns, and elastic travel demands. On the other hand, microscopic traffic simulation is widely used in the transportation engineering field, including transportation system design, traffic operations, and management alternative evaluation. Hence, simulation-based investigation on toll-based traffic operations is of practical importance for traffic professionals to quantify toll impacts, optimize tolling strategies, and identify potential problems prior to implementation.

VISSIM is one of the most powerful microscopic simulation tools developed to model urban traffic and public transit operations. This software can simulate and analyze traffic operations under a broad range of scenarios. In VISSIM, four driving modes are defined: free driving, approaching, following, and braking (Wiedemann 1974 and 1991), and individual vehicle behaviors can be simulated independently (PTV 2007). Many simulation studies have been conducted using VISSIM. Gomes et al. (2004) developed and calibrated a VISSIM model for simulating a congested freeway. Lelewski et al. (2003) built up a VISSIM simulation model to analyze express toll plaza operations. Zhang et al (2008 and 2009) conducted simulation-based investigation on HOT lane operations for Washington State Route 167. Although VISSIM is widely utilized for freeway modeling (Gomes et al., 2004), it cannot handle vehicle routing issues resulting from dynamic tolling strategies with its built-in modules. Review of previous studies did not find any published materials describing VISSIM-based traffic simulation with dynamic toll schemes. Therefore, further efforts for enabling VISSIM models to simulate traffic operations under dynamic tolling strategies are highly desired.

One of the most important but often neglected aspects of simulation studies is the proper analysis of simulation experimental results. Many studies (Alexopoulos 2006, Law 2007, Banks et al 2005, and Welch 1983) indicate that the output data from a simulation run are inherently correlated. The classical statistical methods typically assume that the data are Independent and Identically Distributed (IID) and are not applicable to simulation output data analysis. To handle this issue, a statistical method was developed to investigate data autocorrelation and analyze simulation outputs.

In this study, VISSIM-based simulation testbeds will be developed to simulate toll-based traffic operations and evaluate toll impacts on freeway travel. Two toll facilities in Washington, the SR-167 HOT Lanes and the SR-520 Evergreen Point Bridge, are chosen as the study sites. VISSIM models were built for these two sites as the simulation testbeds in this research project for future investigations of toll strategies.

1.2 Research Objectives

The objectives of this study included the following:

- To build simulation testbeds through customized external module developments for toll strategy investigations;
- To propose a practical calibration process capable of iteratively adjusting traffic demands and driving behavior parameters for strengthened the simulation creditability;
- To develop a statistical method to investigate data autocorrelation and robustly analyze simulation outputs; and
- To apply the simulation testbeds and data analysis method to the two study sites, and research toll impacts on travel patterns and utilization efficiencies of related infrastructures.

CHAPTER 2 LITERATURE REVIEW

2.1 Congestion pricing

Individual travelers impose delays onto others by creating trips, and thus generate a negative externality (De Palma and Lindsey, 2011). The standard economic prescription on the costs of a negative externality is a Pigouvian tax. Pigou (1920) argued to pay for the congestion and thereby launched the study on congestion pricing.

In the past several years, many studies have been conducted to investigate toll impacts on traffic operations and explore optimal toll settings in transportation networks. Marlon and Chalermpong (2001) studied traffic operations of the toll roads in Orange County, California, based on the hedonic models. DeCorla-Souza and Kane (1992) discussed the economic reason for road pricing and impacts of peak period tolls on congestion, air quality, and economic development. Parasibu (2005) discussed the impact of toll roads on regional development in his case study of Jabotabek, the largest urban area in Indonesia. He emphasized the importance of private capital in developing toll roads. Kalmanje and Kockelman (2005) assessed the impact of toll roads in the Austin, Dallas/Fort Worth, and El Paso metropolitan planning areas. They analyzed differences in network configuration, spatial and temporal variations in demand, and road rider characteristics between these regions. De Palma et al. (2005) analyzed time varying tolls in a network using a dynamic network equilibrium simulator. Zhang and Ge (2004), Verhoef (2002 and 2005), and Yan and Lam (1996) also studied imposing tolls on a subset of roadway segments in a network. The results from these studies provided some basic ideas on the toll impact research and are useful for further investigation.

De Palma and Lindsey (2011) summarized three type charging schemes: flat toll, time-of-day toll (Chew, 2008), responsive or dynamic toll (Zhang *et al.*, 2008). Basically, flat tolls are suitable for maximizing revenue whereas time-of-day or dynamic tolls are used for controlling congestion (De Palma and Lindsey, 2011).

Time-of-day toll is defined by the level of toll in each time step. Dynamic toll change its toll rate in response to the real-time traffic condition. Existing research on dynamic tolling algorithms is still in its early stage. In practice, rough dynamic tolling strategies have been executed in several states for HOT lane operations. For example, the toll rate varies from $0.50 to $4.00 for I-15 HOT lanes in San Diego according to different time periods of the day. The tolls may be adjusted in response to real time traffic conditions. The maximum value of \$8.00 is employed for heavily congested situations (Yin and Lou, 2007). Another example is that the tolls of I-394 MnPass Express lane in Minnesota are adjusted upward or downward to maintain the HOT lane travel speed at about 50-55 mph. The tolls range from 25 cents to \$8 and average \$1 to \$4 during peak hours (Zmud et al., 2007). Although the tolling approaches in I-15 and I-394 can be approximately considered as response-based toll adjustment, there are not sufficient theoretical basis supporting them to be reasonably configured and it may not achieve the optimal system performance quantitatively.

Most existing literature on tolling did not provide a systematic and applicable approach for dynamically determining toll rate for tolling system. Chu, Nesamani, and Benouar (2007) proposed a priority-based operation framework for HOV lane usages based on vehicle occupancy, type, and toll rate. However, there was no further investigation on dynamic tolling strategies in their research. Yin and Lou (2007) proposed two approaches to determine dynamic toll. The first one used the concept from the ramp metering control algorithm, ALINEA (Papageorgiou, 1997). By replacing metering rates with toll rates, the control logic of HOT lane management can be expressed as:

$$r(t+1) = r(t) + K \cdot (o(t) - o^*) \tag{2.1}$$

where, $r(t)$ and $r(t+1)$ are the toll rates at interval t and $t+1$, respectively; $o(t)$ is the measured occupancy at interval t; K is the regulator parameter which determines the control strength; o^* is the desired or optimized occupancy of the HOT lane. The other approach utilized a route choice model, the Logit model, to determine the toll rate. The majority of their work was focused on parameter estimation and model calibration using real-time traffic volume from both HOT and GP lanes.

Although previous studies (Appiah and Burris 2005; Halvorson, *et al.* 2006; Yin and Lou 2007; Zmud, *et a*l. 2007) have conducted to evaluate the practical HOT lane systems, research on HOT lane operations is still in its early stage, and a series of theoretical and practical issues on optimizing HOT lane system performance have yet to be addressed.

2.2 Simulation Models for Congestion Pricing Evaluation

Simulation model is used to evaluate the toll impact on the freeway travel in this project. VISSIM is one of the most powerful simulation tools developed to model urban traffic and public transit operations. This software can simulate and analyze traffic operations under a broad range of scenarios. It is also very useful for evaluating various alternatives using the Measures of Effectiveness (MOEs) in transportation engineering and planning (PTV 2011).

In VISSIM, four driving modes are defined: free driving, approaching, following, and braking (Wiedemann 1974 and 1991), and individual vehicle behaviors can be simulated independently (PTV 2011). Besides its standard built-in modules, VISSIM offers COM interfaces for executing COM commands from external programs (PTV 2011).

VISSIM 5.30 also has a Car2X module that can be used to simulate the behavior of connected vehicles (PTV 2011). Car2X module can be used to simulate vehicles receive message and change their driving behavior accordingly, like routing decision (PTV 2011). However, the Car2X module could not be used to simulate the driving behavior under dynamic tolling directly. Further development and adjustments on the Car2X module is necessary.

Another key issue for simulation is that simulation model needs to be carefully calibrated before it can be used for evaluation purposes (Zhang *et al.*, 2008). In VISSIM, traffic flow is modeled as a discrete and stochastic process, in which each driver-vehicle-unit is treated as a single entity. The freeway car-following logic uses the Wiedemann 99 Model (PTV 2011; Wiedemann 1991) and involves ten parameters, including standstill distance, headway time, etc. A detailed driving behavior calibration procedure for freeway operations was described in Gomes' research (2004). Zhang *et al.(*2009) also proposed calibration procedure considering traffic volume and speed. In their study, three major parameters: standstill distance, headway time, and minimum lane changing headway, are adjusted according to the observed field headway data.

After the simulation model is implemented, a proper analysis of the simulation experimental results is of crucial importance for generating meaningful conclusion. This issue is often neglected in a lot of simulation-related studies. When a study needs to analyze the performance of a roadway, normally, multiple simulation runs with different random seeds would be performed. It would be important to accurately estimate the interval that the MOE falls from the multi-run to draw any conclusions about the performance. Use speed data measured from multiple simulation runs as an example. Assume $S_{1i} \quad S_{ji} \quad \cdots \quad S_{ni}$ are IID random variables with the mean μ and variance σ^2.

$$\hat{\mu} = \bar{S}(n) = \frac{\sum_{j=1}^{n} S_{ji}}{n} \tag{2.2}$$

and

$$\hat{\sigma}^2 = S^2(n) = \frac{\sum_{j=1}^{n} (S_{ji} - \bar{S}(n))^2}{n-1} \tag{2.3}$$

The classical statistical methods would construct the Confidence Interval (CI) for the output assuming that μ is the unbiased estimator of the population mean, and is σ^2 the unbiased estimator of the population variance. And thus, an approximate100 (1-α) percent confidence interval for μ can be calculated as:

$$\bar{S}(n) \pm t_{n-1,1-\alpha/2} * \sqrt{S^2(n)/n} \tag{2.4}$$

where, $t_{n-1,1-\alpha/2}$ is the upper 1-α/2 critical point for a *t*-distribution with *n*-1 degrees of freedom. This confidence interval indicates the reliability of the speed estimate based on output data from multiple simulation iterations. The above construction of CI is valid either under the assumption that the population speed follows a normal distribution or, when the population distribution is unknown, the sample size *n* is large enough, normally more than 30, according to Central Limit Theorem (CLT). However, in practice, due to the cost and time required by multiple simulation runs, it is not always realistic to obtain an ideal sample size by running 30+ simulation runs to fulfill the CLT. Therefore, an applicable statistical approach is necessary to estimate the CI under limited sample size with unknown population distribution. Many studies (Alexopoulos 2006, Law 2007, Banks *et al*., 2005, and Welch 1983) also indicate the output data from one single simulation run are inherently auto-correlated. The classical statistical methods typically assume that the data are Independent and Identically Distributed (IID) and are not suitable to analyze simulation output data from a single random seed (Banks *et al*. 2005). To handle this issue, analytical approach is also needed to investigate the autocorrelation problem in the simulation outputs.

CHAPTER 3 STUDY SITE SELECTION AND DATA COLLECTION

3.1 Test simulation sites

In Washington State, there are two types of toll roads: HOT lane-based, such as the SR-167 HOT Lanes, and Bridge-based, such as the SR-520 Evergreen Point Bridge and the SR-16 Tacoma Narrows Bridge (WSDOT, 2011). SR-167 HOT Lanes and SR-520 Bridge are chosen as the study sites for this research. SR-167 HOT Lanes opened to public since May, 2008 and SR-520 Bridge has been tolled since December 2011 (WSDOT, 2011).

3.1.1 SR-167 HOT Lanes

SR-167 is an important highway and serves as an alternative to I-5, connecting south King and north Pierce counties to the cities of Seattle and Bellevue (WSDOT, 2011).

This study focuses on the HOT lane operations on Northbound SR-167. The aerial map of SR-167 is illustrated in Figure. 3.1 and a sketch of the overall simulation network is shown in Figure 3.2. A simulation model is constructed for the SR-167 corridor between I-405 and SR-18 using VISSIM as a simulation testbed for toll strategy investigations. This simulation model is configured to exactly represent the roadway geometric features of SR-167, including the location of on-ramps and off-ramps, horizontal and vertical curves, weaving sections, the number of lanes and so on.

Five HOT segments are implemented in the VISSIM model from SR-167 & 15th St. SW in Auburm to SR-167 & I-405 Interchange Bridge in Renton. The HOT lane segments are marked in Figure 3.2. Three vehicle categories are considered in this research project: SOVs, HOVs, and trucks. Traffic composition for SR-167 is inputted to the simulation model in the form of three Origin-Destination (OD) Matrices. The morning peak period from 6:00am to 9:00am, is chosen as the simulation time period. To eliminate the initial warm-up period, time period from 6:15am to 9:00am is used to perform output data for analysis.

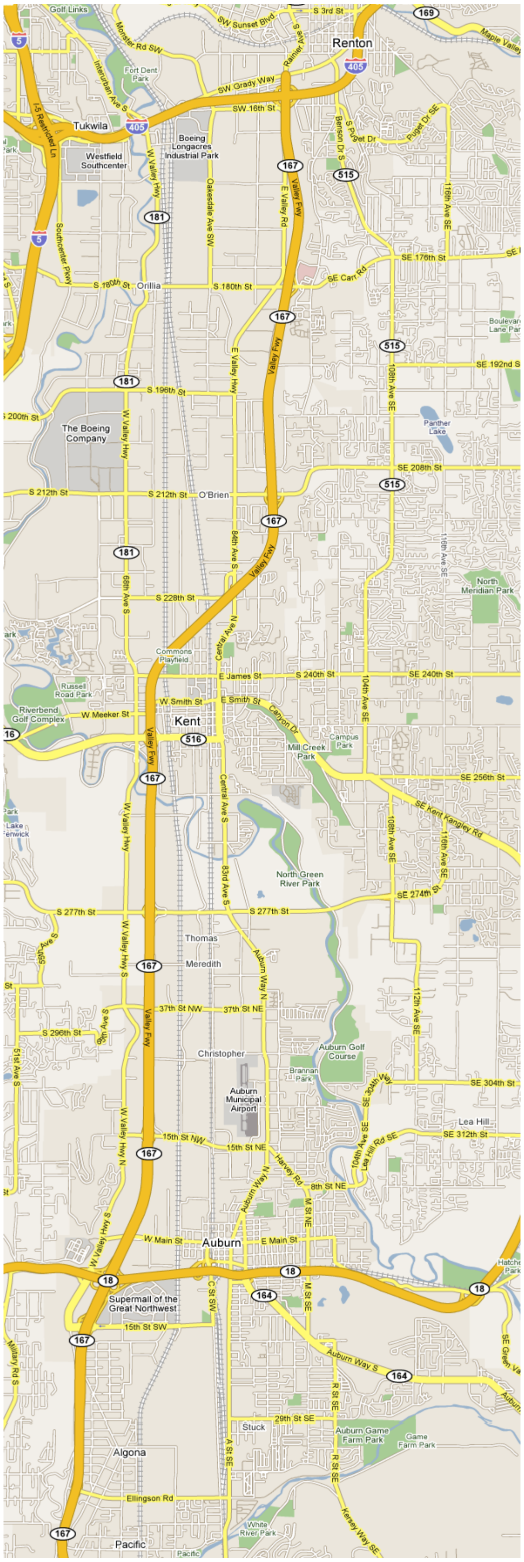

FIGURE 3.1. Aerial map for SR-167

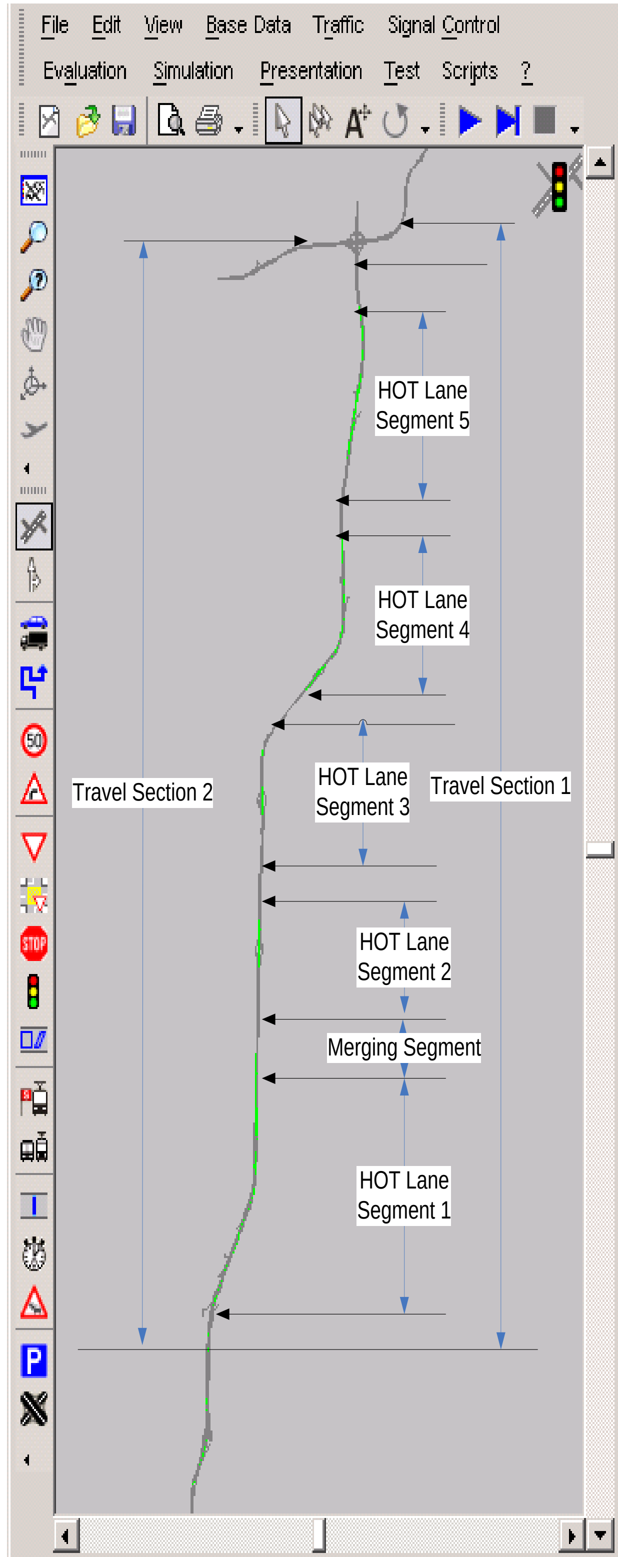

FIGURE 3.2. A sketch of simulation network for SR-167

3.1.2 SR-520 Evergreen Point Bridge

SR -520 and I-90 are the two major corridors across Lake Washington serving east-west traffic between Seattle and Bellevue areas. The SR-520 Evergreen Point Bridge has been tolled since December, 2011, the collected revenue will be used to build a new bridge that is targeted to open in 2014. One key issue that travelers concern about is how the tolling would impact travel of the major freeway network in the Puget Sound area as shown in Figure 3.3. To address this concern, the freeway network of the Puget Sound area encompassing SR-520, I-5, I-90 and I-405 is modeled in this simulation bestbed. Figure 3.4 shows a sketching overview of simulation network for the analysis area.

Table 3.1 presents the WSDOT toll rates schedule at the SR-520 Evergreen Point Bridge for two-axle vehicles during the weekdays. Morning-peak and evening-peak periods have the highest toll rate of up to $3.5 for travelers with *Good to Go!* transponder account. Morning-peak period from 7:7:30am to 8:30am is chosen as the simulation period. The output data from 8:00am to 8:30am are used for analysis.

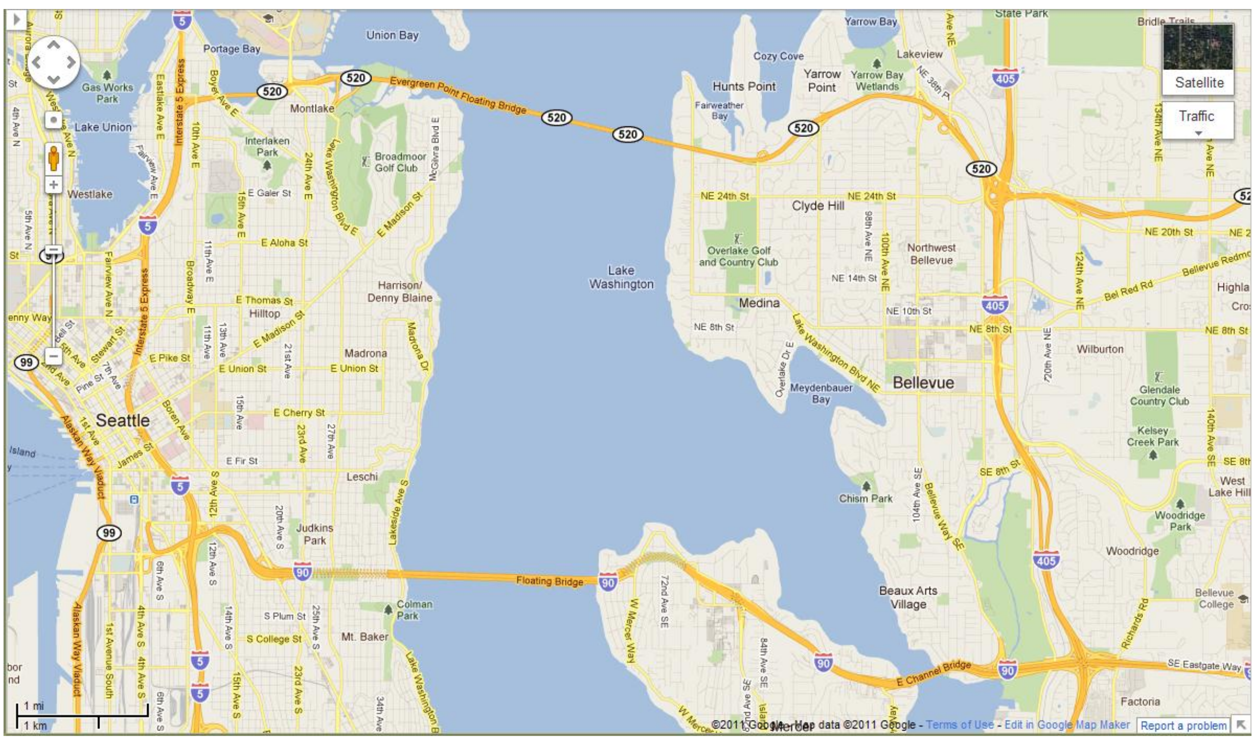

FIGURE 3.3 A geographic map for SR-520 Bridge and I-90 Bridge.

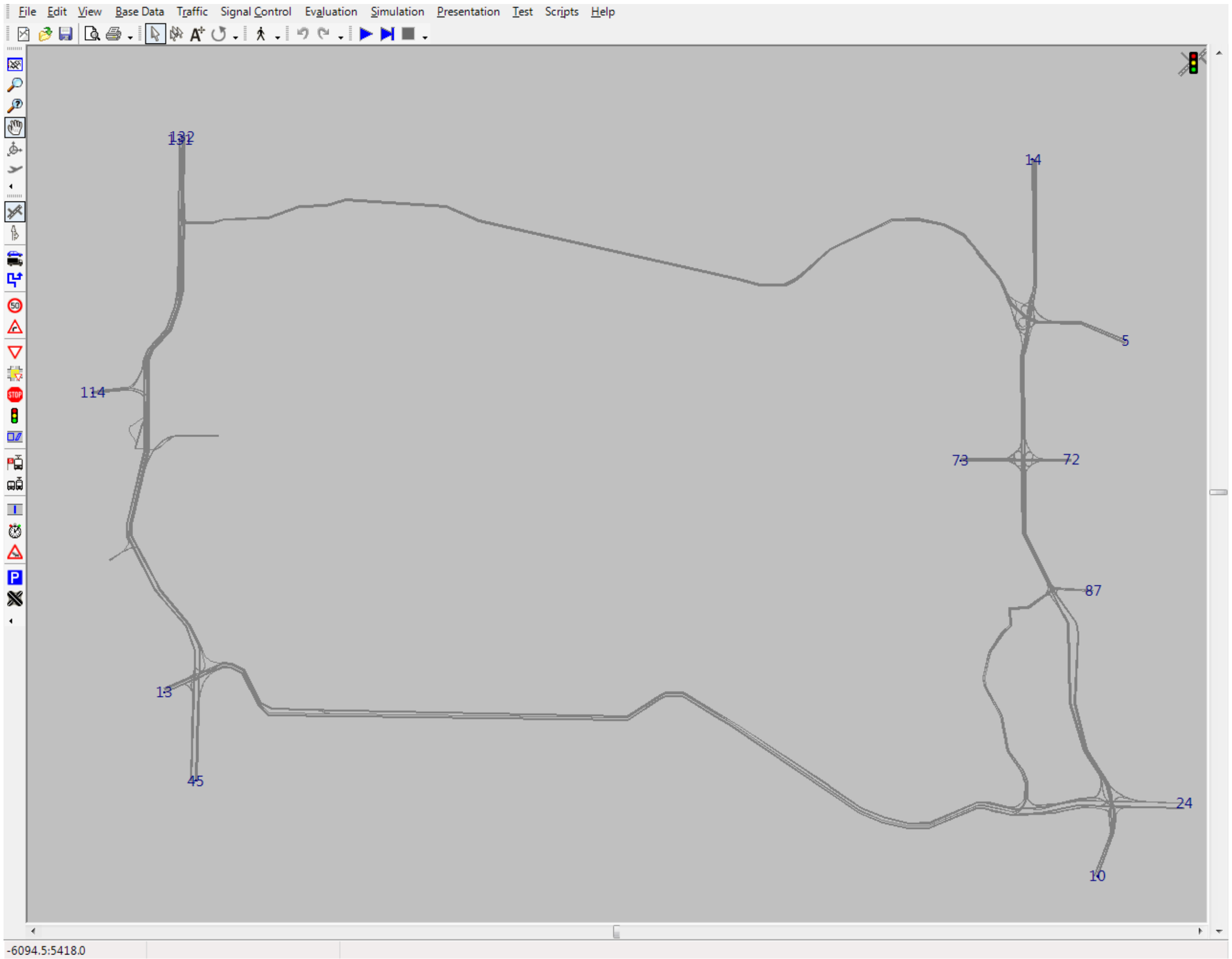

FIGURE 3.4 A sketching overview of simulation network for SR-520 Bridge and I-90 Bridge.

TABLE 3.1 SR-520 toll rates for two-axle vehicles during the weekday (WSDOT, 2011)

Mondays - Fridays	*Good To Go!* Pass	Pay By Mail
Midnight to 5 a.m.	0	0
5 a.m. to 6 a.m.	$1.60	$3.10
6 a.m. to 7 a.m.	$2.80	$4.30
7 a.m. to 9 a.m.	$3.50	$5.00
9 a.m. to 10 a.m.	$2.80	$4.30
10 a.m. to 2 p.m.	$2.25	$3.75
2 p.m. to 3 p.m.	$2.80	$4.30
3 p.m. to 6 p.m.	$3.50	$5.00
6 p.m. to 7 p.m.	$2.80	$4.30
7 p.m. to 9 p.m.	$2.25	$3.75
9 p.m. to 11 p.m.	$1.60	$3.10
11 p.m. to 11:59 p.m.	0	0

3.2 Data

In this study, ground-truth data are collected from two major sources to calibrate and validate the simulation model:

3.2.1 Loop Detector Data

Loop detector data were obtained from WSDOT and archived on a data server called The Digital Roadway Interactive Visualization and Evaluation Network (DRIVE Net) hosted by the STAR Lab at the University of Washington (Ma et al., 2011). Traffic volume data of 20-second intervals on a lane-by-lane basis are available from the data server. Volume data and speed data for all the major routes in the central Puget Sound region, including I-5, I-405, I-90, SR167, and SR-520 are archived and used to calibrate the traffic demand in simulation models. The weekday data without any big incident impact on the freeway is chosen. The data of time period 7am-9am on March 7^{th} (Monday) to 10^{th} (Thursday), is archived and used for simulation experiments.

3.2.2 Report data

Before the simulation model is further used for evaluating the HOT lane operations or toll impact on SR-520, it is important to calibrate the simulation model so that it can replicate the actual scenario of real-world traffic. For calibration purposes, ground-truth traffic data are needed. Three kinds of report data are considered in this study:

- Peak hour report 2010: The Peak Hour Report provided Annual Average Daily Traffic (AADT) and peak hour volume calculated from and including the highest 200 hours of hourly traffic volume. This highest 200 hour traffic volume is collected from Automated Data Collection (ADC) sites being monitored during the previous complete year (WSDOT, 2010). Figure 3.5 shows the data collection sites in the study area for SR-520 Bridge.
- Traffic Management Center Summary Report: SR-167 Ramp and Roadway 2006 Traffic Volumes. This report provides information about hourly traffic volumes on the SR-167 mainline and each ramp. These data play significant roles in calibrating traffic demand inputs.
- SR-167 and I-405 Annual Average Traffic Volumes and Speeds in 2005 (Puget Sound Freeway and HOV Performance Statistics, 2008). This data source offers a favorable dataset of traffic volumes and speeds with a high resolution. Traffic volume is aggregated into 5-min time interval and speeds are measured every half mile along SR-167. These data are important for calibrating driving behavior parameters and network settings.

- OD data. The trip tables provided by WSDOT are the outcomes of the Puget Sound Regional Council (PSRC) four-step planning model (base year 2006). The PSRC base year (2006) model is based on 2006 household activity survey (Cambridge Systematics, Inc, 2007).
- WSDOT Toll Division provided information on how the volume changes on the related freeways after the SR520 bridge being tolled. (Craig et al., 2012)

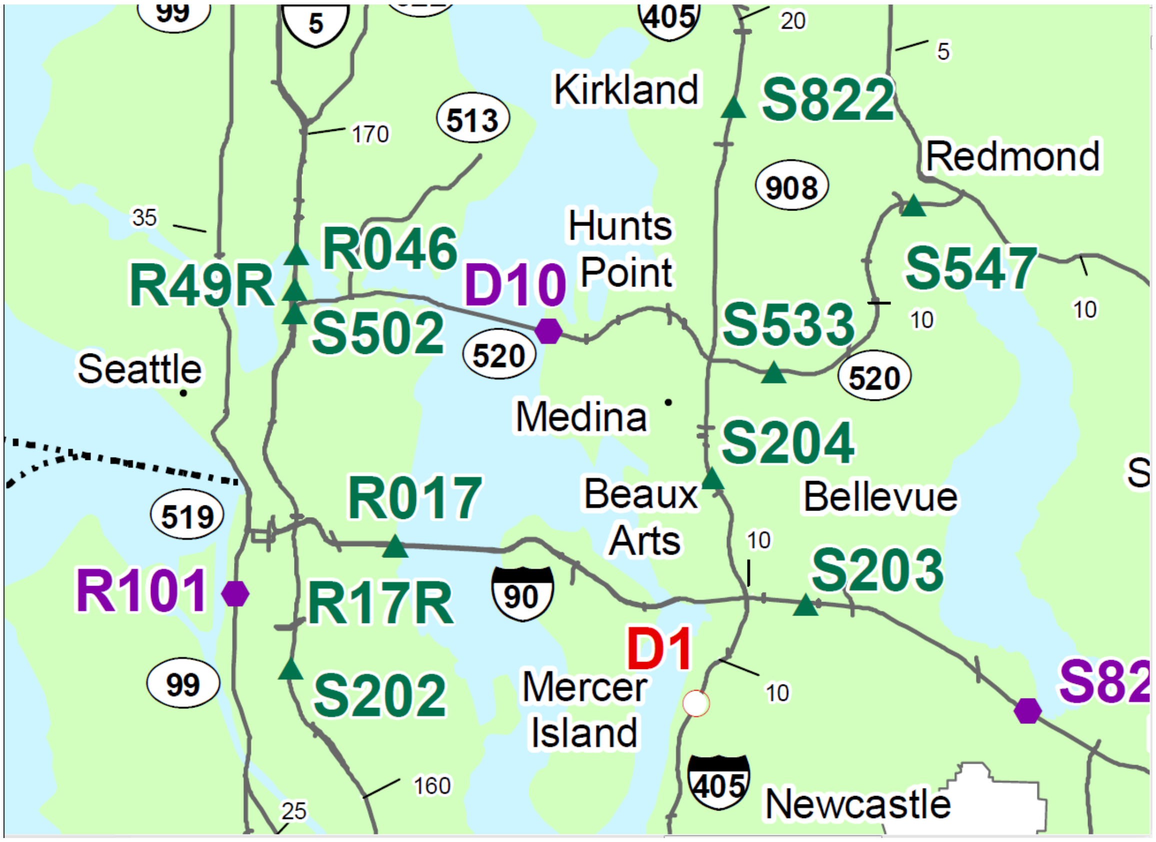

FIGURE 3.5 Data collection sites for center freeway framework of Puget Sound area in the Peak hour report.

TABLE 3.2 Some key location peak hour volume in the study area of the SR-520 Bridge

Site #	Site Location	Milepost	Direction	Peak hour Volume
D10	SR-520 W/O 76TH AVE	MP 4.00	West	3400-3900
S203	I-90 E/O I-405 I/C	MP 10.82	West	5000-5500
S202	I-5 N/O CORSON AVE S	MP 162.35	North	7500-8000
S822	I-405 N/O NE 85th St	MP 18.71	South	5500-6500

CHAPTER 4 RESEARCH APPROACH

The research approach proposed in this study consists of three steps: first, external module will be developed to enable VISSIM models to simulate various traffic operations with complicated tolling schemes; then, a standardized calibration procedure is proposed for freeway traffic simulation to enhance the models' creditability; and finally, a statistical method will be developed to analyze simulation outputs against data autocorrelation problems. The detailed description of each component is expressed as follows.

4.1 External Module Development

Two VISSIM external modules are developed in this research. For the SR-167 HOT simulation, an external tolling control module using COM server is developed to dynamically adjust the optimal toll rate. For SR-520 Bridge simulation, an external routing module using Car2X module is developed to dynamically update vehicle routing.

4.1.1 External Tolling Control Module Using the COM Server

In VISSIM, a static toll rate can be set up as the financial cost for each roadway segment, but it is not dynamically changeable to reflect changing traffic conditions under the flexible tolling strategies required by most toll-based traffic operations. In order to provide sufficient flexibility to implement various toll strategies and realize dynamic vehicle rerouting to respond to traffic condition changes, an independent functional module of VISSIM will be developed. This external module should use standard VISSIM COM interfaces for general applications, and be capable of retrieving real-time traffic information from simulation models. Once developed, it can be easily incorporated in VISSIM simulation models to analyze toll-based traffic operations and evaluate toll impacts under various traffic scenarios and tolling strategies.

Besides its standard built-in modules, VISSIM offers COM interfaces for executing COM commands from external programs (PTV 2007). Such customer-based COM applications provide extensive simulation capacities needed for satisfying various requirements from users. After the VISSIM COM server is registered in the computer operation system, communications between the external program and the VISSIM model are set up. The COM objects, such as individual vehicles, and roadway segments, can be utilized and controlled by external programs. Through a COM interface, an external program can access the VISSIM simulation model to retrieve traffic data and logic decisions. In this study, Microsoft Visual Basic is used as the computer language to implement the tolling control module. The communications between this external module and the built-in modules of VISSIM are shown in Figure 4.1, the overall system architecture of the toll-based traffic simulation testbed.

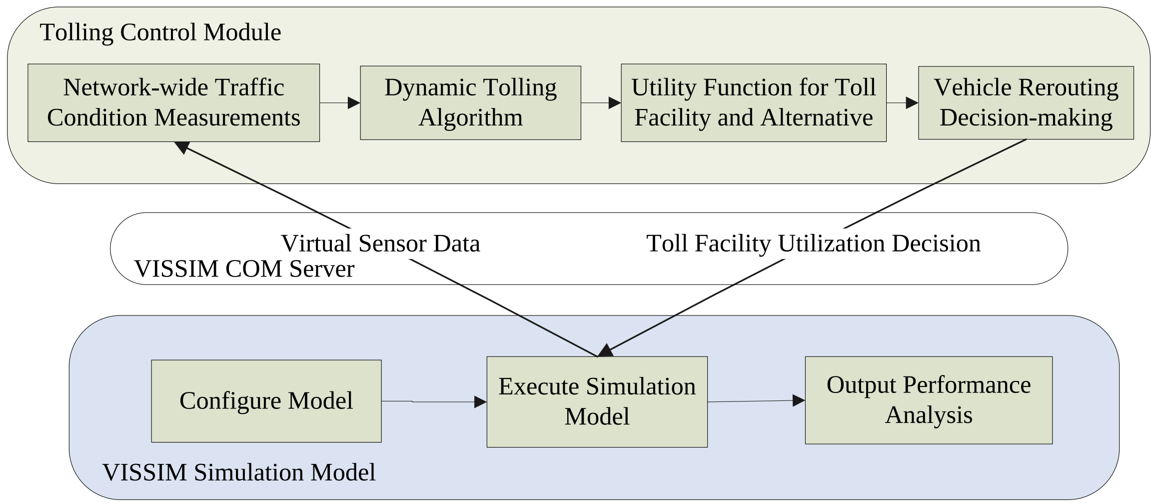

FIGURE 4.1 System architecture of the toll-based traffic simulation testbed.

After the VISSIM simulation model is correctly configured, including accurate geographic characteristics of traffic networks, proper traffic demand matrices, and traffic compositions, etc., the model will be executed in the single-step mode (default frequency: 1 second). When the traffic is allocated into the network by the dynamic assignment module, the flow rates, lane occupancies and speeds are measured by virtual loop detectors in the network. At each single step, these traffic detection data are exported and transferred to the external tolling control module via the VISSIM COM server. These data will be aggregated in a certain interval to synchronize with toll updating intervals. Based on traffic conditions in the network, the tolling algorithm will be executed and the dynamic toll rate determined. Then, the utilization of toll facilities and the alternatives are assessed using the toll rate and these measurements from the simulation model.

In reality, individual motorists will make decisions on whether to pay for using toll freeways based on the real-time toll rate, and traffic conditions on toll freeways and the alternatives. In simulation experiments, we employ a Logit model based on Zhang et al. (2008) to imitate this decision-making process. To quantify the attractiveness of different facilities, the total cost (*TC*) for choosing facility type *i* is computed as

$$TC_i = \alpha * TT_i + TR_i + \beta * TD_i / SP_i \tag{4.1}$$

where, TT_i is the average travel time and TR_i is the toll rate for facility type i; α is the coefficient to convert TT_i into a cash value; TD_i is the travel distance; SP_i is the speed limit; β is the coefficient to balance the specific weight of such static attributes for a freeway segment. For the type of non-toll freeway, the toll rate $TR_{re} = 0$. Then, the utility function U for different choice is calculated as

$$\begin{aligned} U_{toll} &= \frac{1}{TC_{toll}} = \frac{1}{\alpha * TT_{toll} + TR_{toll}} \\ U_{re} &= \frac{1}{TC_{re}} = \frac{1}{\alpha * TT_{re}} \end{aligned} \tag{4.2}$$

where U_{toll} is the utility function of the toll freeway and U_{re} is the utility function of the regular non-toll freeway. Then, the probability of lane choice is formulated by the commonly used Logit model as follows

$$P_{toll} = \frac{\exp(U_{toll})}{\exp(U_{roll}) + \sum \exp(U_{re})} \tag{4.3}$$

where P_{toll} is the probability of choosing the toll freeway for each individual vehicles, also, from a macroscopic perspective, P_{toll} denotes the proportion of vehicles that use the toll freeway. $\sum$ indicates that multiple regular freeways are available, and the sum of the utility functions should be computed. Analogously, the proportion of vehicles choosing the regular freeway can be calculated.

Via the COM interface, each vehicle can be tracked and controlled by the external program. To simulate the probabilistic route decisions for each individual vehicle, a sequence of random numbers, $\{N_j\}$, in the range from 0 to 1 with uniform distribution is generated. The logic decision is conducted as follows:

$$\begin{cases} N_j \le P_{toll} \Rightarrow True \\ N_j > P_{toll} \Rightarrow False \end{cases} \tag{4.4}$$

where j denotes the jth vehicle; the decision *True* indicates when N_j is less than or equal to P_{toll}, the vehicle j will choose the toll freeway; and vice versa. After assigning an individual vehicle to the toll freeway or the regular alternative, this route decision is imported to the VISSIM model to replace its original route decision. Consequently, dynamic toll-based traffic operations can be realized.

Dynamic tolling algorithms can be implemented in this tolling control module to satisfy the unique demands for specific researchers and practitioners. Integrating this module with the standard VISSIM platform, the simulation testbed can be established to simulate toll-based freeway traffic operations under various scenarios, and further evaluate toll impacts on travel patterns and utilization efficiency of traffic infrastructures.

4.1.2 External Routing Module Using Car2X Module

In the SR-167 simulation testbed, an external tolling control module was developed using the COM interfaces. Route choice behavior of each vehicle in this model still follows the path selection process from VISSIM build-in dynamic assignments functionality. In VISSIM, a path is defined as a sequence of nodes, and must begin and end at parking lots. It should be noted that identifying all paths in complex traffic networks could be difficult, and with the increase of the network scale, it becomes even impossible. For the network of which link travel times follows a non-stationary distribution, or said, being stochastic time-variant, the optimal routing strategy of a vehicle is not just searching a simple path for its travel, but making a series of dynamic decision routing (Hall, 1986). A route choice module that is capable of accommodating advance routing strategies, such as dynamic programming, is highly desirable. In the SR-520 simulation testbed, the Car2X module is thus utilized for simulating vehicles route choice behavior after the toll implementation.

The Car2X module is originally designed for simulation of intelligent vehicles that are equipped with wireless communications such as the Connected Vehicle (or CV-cars). Although there are differences between regular vehicles and CV-cars, it is reasonable to assume that current vehicles in the freeway network in reality have certain access to the real-time traffic information to facilitate their routing decisions, such as Variable Message Signs (VMS), traveler information system from smartphone or internet, radio, etc.. The Car2X vehicles can be considered as model of such users.

The Car2X module works in a similar fashion as COM server, but has provided another group of Python/C++ application programming interfaces (APIs) in order to simulate activities like:

- Wireless information sending and receiving; and
- Dynamic driver behaviors, like lane changing and route choice.

The latter functionality is enabled by giving users the freedom of reading and assigning routes ID on static routing decision. During each simulation run, when Car2X vehicles face a routing decision, the API allows them to update their desire routes based on the real-time traffic conditions. With this feature, the module is capable of updating routing decisions without identifying all the possible paths; and thus it is more flexible for implementing custom routing strategies. A detail comparison between COM API based and Car2X module based routing is shown in the Table 4.1.

TABLE 4.1 Comparison between COM-based and Car2X routing.

	Dynamic Assignment with COM Server	Car2X module route choice function
Applicable Objects	Vehicles with route guidance equipment	Vehicles with Car2X equipment
Vehicle Inputs	OD matrix (.fma file)	Static vehicle inputs or OD matrix
Route Choices	Paths (as sequences of nodes)	Paths or routes in static routing decisions
Allowing Routing Updates?	Yes, but all the paths need to be defined first.	Yes, when objects get in routing decisions.

The communications between the external modules and the built-in modules of VISSIM are shown in Figure 4.2. The execute simulation model will call Car2X module and COM interface at each time step. The real time traffic conditions and other information, such as users' OD and knowledge about the network, are feeding into the vehicle routing behavior module. In SR-520 tolling testbed, the network has been divided into several segments based on the distribution of on ramps and off ramps. Figure 4.3 shows the eight segments used for routing for SR-520 Bridge tolling simulation. An external COM module is also implemented for acquiring the speed detection result from sensors in the network. Based on the detection results and segments static information, instant segment travel cost is calculated and then route choices are made based on utility functions.

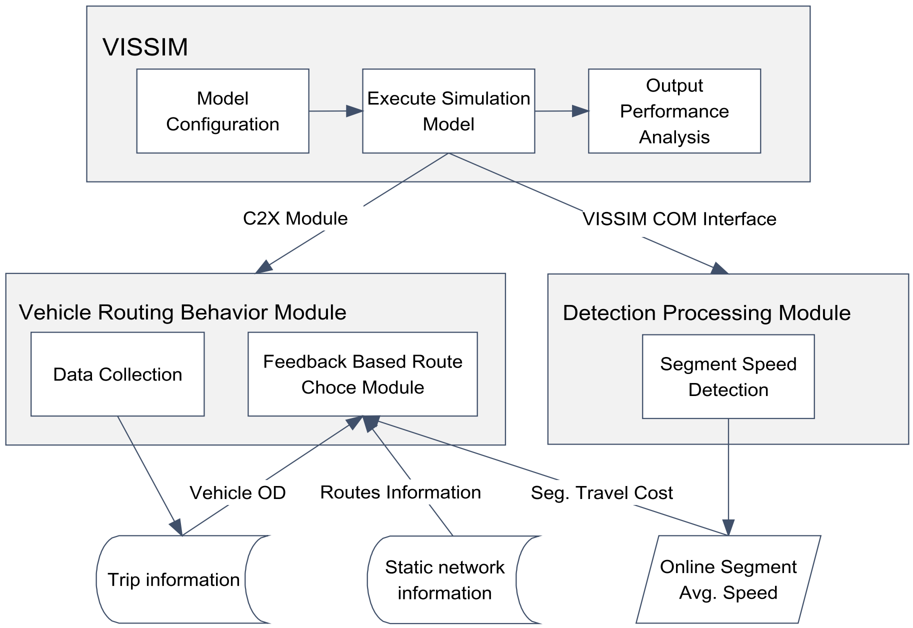

FIGURE 4.2 System architecture of the external routing module.

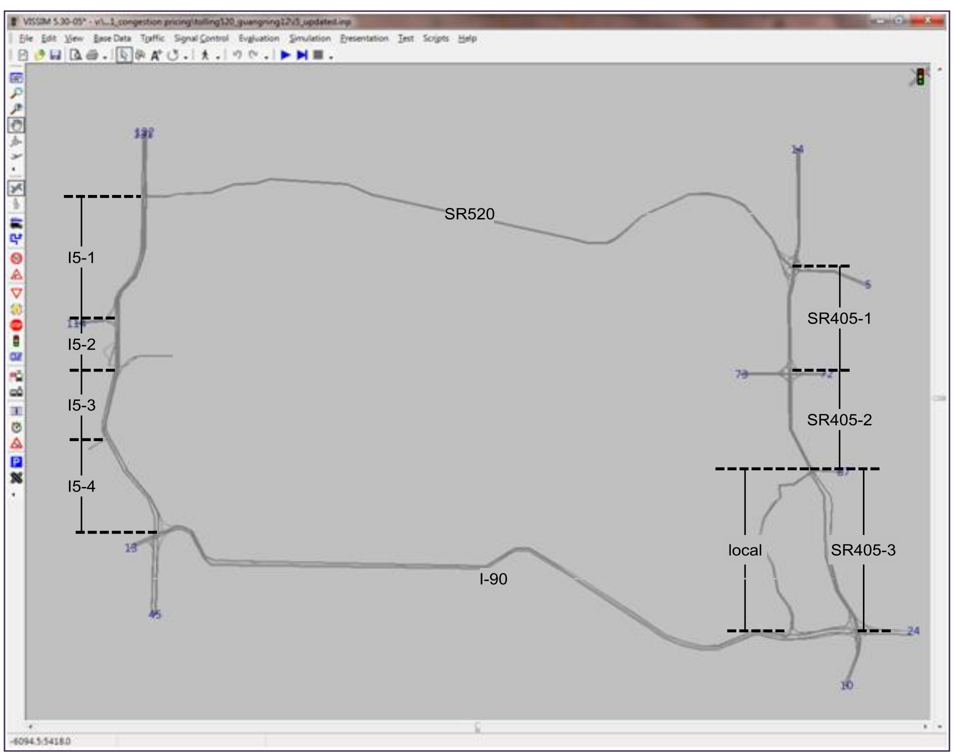

FIGURE 4.3 Simulation segments in the network.

4.2 Simulation Model Calibration

Simulation model calibration is crucial to ensure realistic representations of simulated scenarios and achieve reliable simulation results. Calibration efforts are required for reasonable correspondence between observed field data and simulation outputs. During the model calibration process, related parameters are adjusted to make the outputs practically represent field conditions. The schematic flow chart of the proposed calibration procedure is illustrated in Figure 4.4.

With its built-in dynamic assignment module, VISSIM can dynamically assign and equilibrate traffic in the network based on the demand of trips from origins to destinations. In VISSIM, a set of possible routes between two zones are established, and then travel costs (e.g. travel time, toll and distance) for each route are calculated. Based on the assessment of optional routes, a discrete choice model is exploited to allocate traffic demands on all possible routes to model the route choice behavior of drivers. Such assignment processes are iterated dynamically until traffic assignment reaches the equilibrium status. By using the dynamic traffic assignment, the proposed simulation testbed is capable of simulating present traffic operations appropriately. For calibration purposes, ground-truth data including traffic flow rates and speeds at a series of important check points in the network are needed.

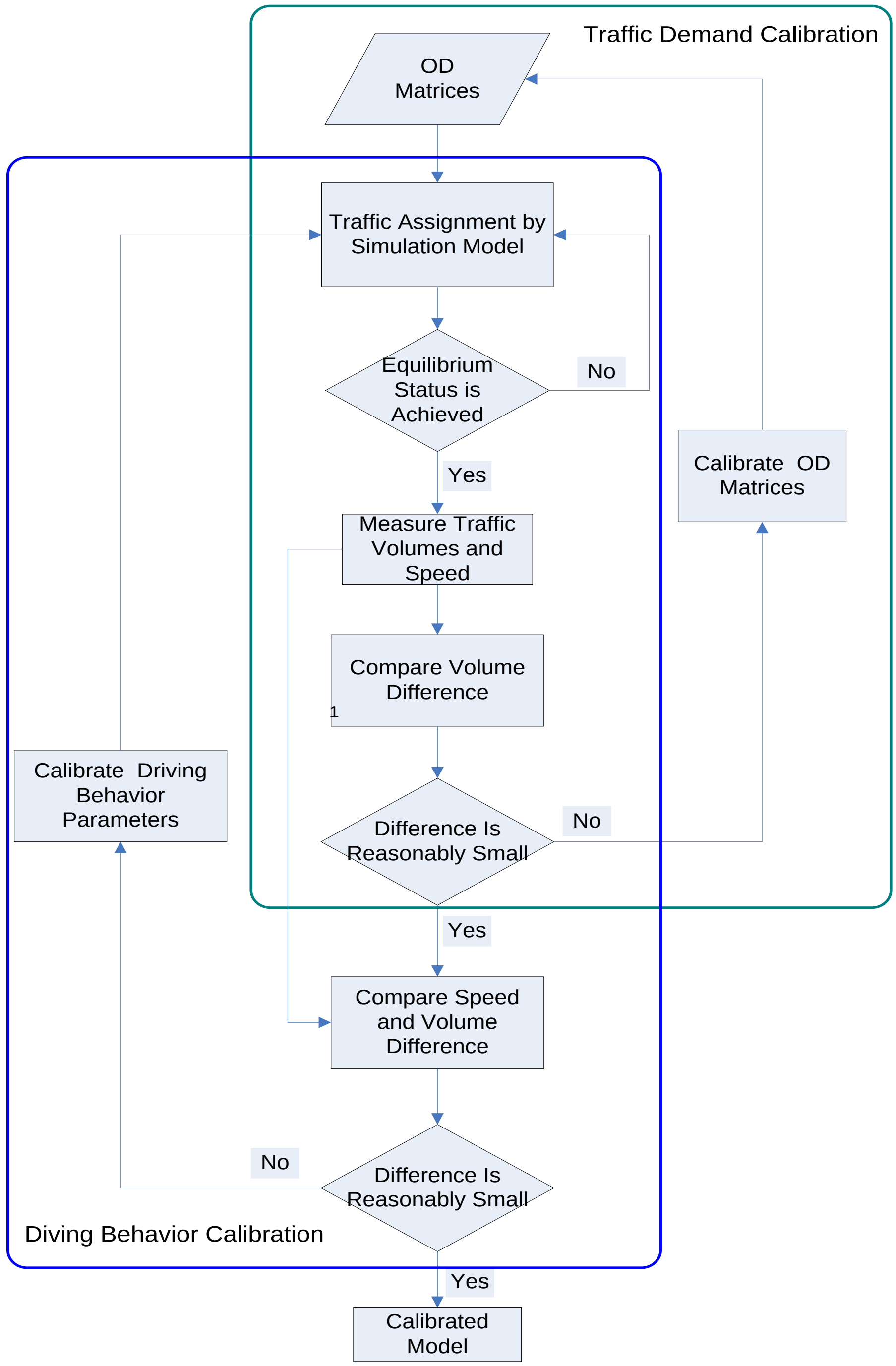

Figure 4.4 Schematic flow chart of the calibration procedure.

The proposed calibration procedure is composed of two iterative subroutines: traffic demand calibration and driving behavior parameter calibration. First, traffic demand calibration will be performed. Based on the traffic planning survey data, traffic trip matrices are established and inputted to the simulation model. Through multiple iterations of traffic assignment, these traffic demands are allocated to the whole network and the assignment equilibrium is achieved. To check the fidelity of this simulation model, virtual loop sensors are placed in the simulation model according to their real positions on ramps and freeway corridors. Traffic counts and speeds are collected from these virtual loop detectors and compared to the reference data. If they are significantly different, then trip attraction and production in the OD matrices are rebalanced so that the difference can be reduced. These steps are iterated until the volume difference is reasonably small (less than 10%).

Then driving behavior parameter calibration is conducted using the traffic volume and speed data. In VISSIM, traffic flow is modeled as a discrete and stochastic process, in which each driver-vehicle-unit is treated as a single entity. The freeway car following logic uses the Wiedemann 99 Model (PTV 2007; Wiedemann 1991) and involves ten parameters, including standstill distance, headway time, etc. In this study, three major parameters: standstill distance, headway time, and minimum lane changing headway, will be carefully adjusted according to the observed field headway data. Also, other parameters, such as the look-back distance, etc. are modified individually for weaving areas. A detailed driving behavior calibration procedure for freeway operations can be found in Gomes' research (2004). After tuning up these parameters, the simulation model is iteratively executed until traffic assignment is equilibrated in the network. Based on the comparisons between the simulation results and the corresponding reference data, such calibration processes are repeated. Once the difference is small enough at multiple check points, the testbed is considered reasonably calibrated and is ready for toll traffic simulation.

4.3 Simulation Output Analysis

4.3.1 Interval Estimates from Multiple Simulation Runs

In many existing transportation simulation studies, a great amount of time and money is invested in model development with little effort made to analyze simulation outputs appropriately. Because of the randomness in the components driving a simulation, the outputs from simulation models are statistical variables. So statistical techniques should be used to analyze the simulation output data and obtain the models' true characteristics.

As a matter of fact, simulation models utilize the pseudo-random number sequence to emulate the randomness in reality. The variations in different random seeds would affect the realization of the stochastic quantities in VISSIM, such as inlet flows and vehicle capabilities. In practice, at least five seed runs are generally recommended for congested corridors to conclude the generality of the simulation result. However, very few studies have been performed to analyze the output sensitivity towards different number of random seeds.

In this research project, methods for interval estimation from multiple random seed runs and single simulation runs are proposed. If $\{Y_1, Y_2, \ldots, Y_n\}$ are statistically independent observations, which is the case for the datasets at the same time intervals from multiple random seeds, classical statistical methods can be applied. Output data from a single simulation run, on the other hand, are intrinsically correlated. Hence, classical statistical methods may not be suitable to use directly due to their strict assumptions of IID variables. Additionally, because random samples from a certain probability distribution are typically utilized in simulation, output data from a single simulation run are just particular realizations of random variables, potentially introducing large variances.

For simulation outputs, there are primarily two types of performance measures: transient performance measures, and steady-state performance measures (Law, 2007). Our study will concentrate on traffic operation analysis under stabilized conditions using steady-state performance measures. For the sake of simplicity, we use the speed data as an example to demonstrate the proposed analysis procedure. After traffic is allocated to the network and reaches the equilibrium status, the average speed data which are aggregated in 15-min intervals are measured along a particular freeway section. The data matrix can be expressed as follow

$$\begin{matrix} S_{11} & \cdots & S_{1i} & \cdots & S_{1m} \\ \vdots & & \vdots & & \vdots \\ S_{j1} & \cdots & S_{ji} & \cdots & S_{jm} \\ \vdots & & \vdots & & \vdots \\ S_{n1} & \cdots & S_{ni} & \cdots & S_{nm} \end{matrix} \tag{4.5}$$

where, S_{ji} is the average speed for the *ith* 15-min interval from the *jth* simulation run; $\begin{bmatrix} S_{j1} & S_{j2} & \cdots & S_{jm} \end{bmatrix}$ is the realization of the *jth* simulation run with *m* intervals. Obviously, these variables are correlated and are not IID. By changing simulation random seeds, we can obtain the different realizations from different simulation replications. Suppose we have *n* independent simulation replications, and the vector $\begin{bmatrix} S_{1i} & S_{ji} & \cdots & S_{ni} \end{bmatrix}^T$ denotes the speed data sequence of the *ith* interval from

n simulation replications. Because each entire replication is independent of any other replication, and each replication's observations have the same distribution, the variables $S_{1i} \quad S_{ji} \quad \cdots \quad S_{ni}$ are indeed IID observations. This independence across different simulation runs will be exploited as complement information to draw inferences about simulation outputs.

When statistics are computed from a randomly chosen sample, then these statistics are random variables. Methods of statistical inference such as Confidence Intervals (CIs) and hypothesis tests are predicated on the randomness of statistics. For example, the confidence coefficient of a confidence interval tells us the probability, before a random sample is taken, that an interval constructed from the sample will contain the parameter. One of the most prevalent statistical methods for data analysis is the confidence interval test. Information about the precision of estimation is conveyed by the length of the interval. A short interval implies a precise estimation. One cannot be certain that the interval contains the true, unknown population parameter, however, one can use a sample from the full population to compute the point estimate and the interval. The confidence interval is thus constructed so that we have high confidence that it does contain the unknown population parameter. Suppose we wish to construct a confidence interval for the population mean based on a random sample. It requires a method of estimating the variance of the point estimator in a unbiased fashion. For the speed data measured from multiple simulation runs, $S_{1i} \quad S_{ji} \quad \cdots \quad S_{ni}$ are IID random variables with the mean μ and variance σ^2. The unbiased point estimators for μ and σ^2 are expressed as follows

$$\hat{\mu} = \bar{S}(n) = \frac{\sum_{j=1}^{n} S_{ji}}{n} \tag{4.6}$$

and

$$\hat{\sigma}^2 = S^2(n) = \frac{\sum_{j=1}^{n} (S_{ji} - \bar{S}(n))^2}{n-1} \tag{4.7}$$

An approximate 100(1-α) percent confidence interval for μ can be calculated as

$$\bar{S}(n) \pm t_{n-1,1-\alpha/2} * \sqrt{S^2(n)/n} \tag{4.8}$$

where, $t_{n-1,1-\alpha/2}$ is the upper 1-α/2 critical point for a t-distribution with n-1 degrees of freedom. This confidence interval indicates the reliability of the speed estimate based on output data from multiple simulation iterations. The above construction of confidence interval is valid under the assumption that the population speed follows a normal distribution. It is also valid for the scenario that S_{1i} S_{ji} $\cdots$ S_{ni} are a series of random sample from a population with unknown distribution and the sample size n is large. Then the CLT implies that $\bar{S}(n)$ has approximately a normal distribution with mean μ and variance σ^2/n.

However, in practice, due to the cost and time required by multiple simulation runs, it is not always realistic to obtain an ideal sample size by running 30+ simulation runs to fulfill the CLT. So for the limited sample size, can we still get a confidence interval? The answer is "yes, by resampling."

There are two basic resampling methods, model-free and model-based, which are also known, respectively, as nonparametric and parametric (Ruppet, 2011**)**. In model-free resampling, the resamples are drawn with replacement from the original sample. That is because only sampling with replacement gives independent observations, and we would expect the resamples to be IID observations just as the original sample. For the model-based resampling, it does not take a sample from the original sample. Instead, it is assumed that the original sample was drawn IID from a density in the parametric family. The resamples are drawn IID from the density as well.

In this research project, a computer simulation technique called "bootstrap" is applied to find the confidence interval. Bootstrap is a model-free resampling approach. It is one way that modern computing has revolutionized statistics.

Assume that we have $\boldsymbol{B}$ number of resamples from the original sample. Let $\bar{Y}_{boot,b}$ and $s_{boot,b}$ be the sample mean and standard deviation of the bth resample, b=1,….$\boldsymbol{B}$, and let $\bar{Y}$ be the mean of the original sample. We can define

$$t_{boot,b} = \frac{\bar{Y}-\bar{Y}_{boot,b}}{s_{boot,b}/\sqrt{n}} \tag{4.9}$$

From Equation 4.9, it is noticed that for the resample, the population mean is $\bar{Y}$. That is to say, a resample is taken using the original sample as population. Because the resamples are independent of each other, the collection of $t_{boot,1}, t_{boot,2}\ldots$ can be treated as a random sample from the distribution of t-statistics. After $\boldsymbol{B}$ values of $t_{boot,b}$ have been calculated, we can find the $\alpha/2$-lower and –upper quantiles of these $t_{boot,b}$ values, called t_L *and* t_U. Now we replace the $\pm t_{n-1,1-\alpha/2}$ in Equation 4.8 by t_L *and* t_U, respectively. Finally the bootstrap confidence interval for μ is

$$(\bar{S}(n)+t_L*\sqrt{S^2(n)/n},\ \bar{S}(n)-t_U*\sqrt{S^2(n)/n}) \tag{4.10}$$

In Equation 4.10, $\bar{S}(n)$ and $S^2(n)$ are the mean and variance of the original sample, and only t_L *and* t_U are calculated from the ***B*** bootstrap resamples.

4.3.2 Interval Estimates from Single Simulation Run

If $\{Y_1, Y_2, \dots, Y_n\}$ are not statistically independent, which is the case for the dataset from one single simulation run, $S^2(n)/n$ is then a biased estimator of the true variance. In this situation, $\{Y_1, Y_2, \dots, Y_n\}$ is an autocorrleated sequence, sometimes called time series. To estimate the CI from the time series, we use 15-min speed data, $S_{j1} \quad S_{j2} \quad \cdots \quad S_{jm}$, from the *jth* simulation run as an example. Although these variables are correlated, the sample mean $\bar{S}(m)$ is an unbiased estimator of μ still. But the sample variance $S^2(m)$ is no longer an unbiased estimator of σ^2. Therefore, the variance should be calculated as

$$Var(\bar{S}_M) = \frac{Var(S_1 + S_2 + \cdots + S_M)}{M^2} = \frac{1}{M^2}\sum_{h,g=1}^{M}\mathrm{cov}(S_h, S_g) \tag{4.11}$$

where, $\mathrm{cov}(S_h, S_g)$ denotes the covariance between variables S_h, and S_g; which is a measure of their dependence. $\mathrm{cov}(S_h, S_g)$ can be calculated as

$$\mathrm{cov}(S_h, S_g) = E[(S_h - \mu)(S_g - \mu)] = E(S_h S_g) - \mu^2 \tag{4.12}$$

We assume the measured speed data are steady-state variables, so the covariance $\mathrm{cov}(S_h, S_g)$ is only associated with the difference between h and g. Also note variances are symmetric such that $\mathrm{cov}(S_h, S_g) = \mathrm{cov}(S_g, S_h)$. Assume $k = g - h$, so Equation (4.11) can be calculated further

$$
\begin{aligned}
Var(\bar{S}_M) &= \frac{1}{M^2}\sum_{h,g=1}^{M}\operatorname{cov}(S_h, S_g) = \frac{1}{M^2}\sum_{h,g=1}^{M}\operatorname{cov}(h-g) \\
&= \frac{1}{M^2}[M\operatorname{cov}(0) + (M-1)\operatorname{cov}(1) + (M-1)\operatorname{cov}(-1) + \cdots + \operatorname{cov}(M-1) + \operatorname{cov}(1-M)) \\
&= \frac{1}{M^2}\sum_{k=-M}^{M}(M-|k|)\operatorname{cov}(k) \\
&= \frac{1}{M}(\operatorname{cov}(0) + 2\sum_{k=0}^{M-1}(1-k/M)\operatorname{cov}(k)
\end{aligned}
\tag{4.13}
$$

Based on Equation (4.12), cov (*k*) can be calculated as

$$
\operatorname{cov}(k) = \frac{1}{M-k}\sum_{l=1}^{M-k}(S_l - \mu)(S_{l+k} - \mu) \tag{4.14}
$$

Combining Equation (4.13), (4.14), and (4.10), the 100(1-α) percent confidence interval for auto-correlated data of simulation outputs can be obtained:

$$
\bar{S}(m) \pm t_{m-1,1-\alpha/2} * \sqrt{Var(\bar{S}_M)} \tag{4.15}
$$

Analogously, the proposed analysis procedure is suitable for significance tests comparing different sample data sets under various simulation scenarios. It can sufficiently handle the data correlation problems and strengthen simulation outputs' reliability.

CHAPTER 5 SR-167 HOT LANE TESTBED

In order to compare the impacts of different tolling strategies on the freeway travel, three operational schemes are considered in this research project:

- HOV Lane Operation (Strategy I): SOVs are restricted from using the HOV lane;
- HOT Lane Operation with Time-of-day Toll Rate (Strategy II): SOVs could use HOT lane in exchange of travel time savings if they are willing to pay a toll. The toll rate is changed based on a fixed time-of-day schedule; and
- HOT Lane Operation with Dynamic Toll (Strategy III): SOVs could use HOT lane in exchange of a travel time saving if they are willing to pay a toll. And the toll rate is dynamically changed based on the real-time traffic condition.

The peak-hour traffic demands from 6:00-9:00am collected at the SR167 HOT lane corridor in Puget Sound serve as the base scenario. Two other scenarios, 80% and 120% of the current demands, are tested as well. This is to provide a platform of testing the effectiveness and the robustness of different operational/tolling schemes through the evaluation of system performance.

Data used for simulation network performance evaluation are extracted from 6:15 am to eliminate the initial warm-up period. To accommodate the randomness of simulation results and enhance simulation models' credibility, each simulation scenario is conducted under multiple random seeds. Three MOEs, travel time, traffic throughputs, and traffic speed (space-mean speed) are used as the performance indicators. These three indicators are compared amongst different operational strategies in Sections 5.1 and 5.2. A detail comparison on speed within each segment on the SR-167 site is discussed in Section 5.3. The impacts on the overall network from different operational strategies are discussed in Section 5.4.

5.1 HOV Operation vs. HOT Operation

The simulation experiments were conducted under six conditions:

a. HOV operation under existing traffic Demands
b. HOV operation under 80% of the current traffic Demands
c. HOV operation under 120% of the current traffic Demands
d. HOT operation with dynamic toll under existing traffic Demands
e. HOT operation with dynamic toll under 80% of the current traffic Demands

f. HOT operation with dynamic toll under 120% of the current traffic Demands

The aggregated simulation results for HOV operation and HOT operation with dynamic toll under existing traffic demands are summarized in Table 5.1. It includes performance measures of travel time, throughputs, and traffic speeds for the entire system. The last two columns are the improvement ratios between two operational strategies. The throughput difference between the HOT lane system and HOV lane system is divided by the throughputs of the HOV lane system. This ratio is defined as the throughput improvement. Similarly, an analogous variable is defined for traffic speed and is shown in the last column of Table 5.1.

Based on the results shown in Table 5.1, the improvement across of the cross section of the freeway (GP+HOV/HOT) is significant. The improvement on the throughput is ranged from 1% to 10% for the five segments, whereas the improvement on the speed is ranged from 10% to 80% for the five segments. Note that Segment 4 has the biggest improvement in throughput, changed from 6,252 to 6,905 vehicles within the simulation time period. Segment 1 has the biggest improvement in speed, where the average speed enhanced from 29.5 mph to 53.7 mph within the simulation time period.

The benefit of the HOT operation is quite pronounced. For example, in Segment 1, under HOV operation, the average speed of GP lanes is 27.3 mph, and that of HOV lane is 59.6 mph. The average speed across the entire segment's cross section is about 29.5 mph. Under HOT lane operations, the number of vehicles choosing to use the HOT lane increases from 791 to 2,184 within the simulation period, and, as a result, the average speed of the GP lanes increases to 51.0 mph. However, the speed of the HOT lane keeps at the same level, about 58.6 mph and the overall average speed improves to 53.7 mph, an improvement of 82.0%.

The merging areas 2, 3, and 4 have significant improvements under HOT lane operations. For example, under HOV lane operations, the average speed of the merging area 3 is 28.6 mph, whereas under HOT lane operations, the average speed of the same merging area becomes 55.2 mph. The traffic speed on merging area 1 slightly decreases under HOT lane operation. This may due to the fact that more SOVs changed their routing decision and choose the HOT lane under congested situation. The average speed of merging area 5 is 53.7 mph under HOV lane operations. This is because many vehicles are blocked due to the congestion in merging area 4 and Segment 4.

For the on-ramp and off-ramp traffic, as seen in Table 5.1, improvements under HOT operation are significant in all segments. For example, for Segment 2, the on-ramp and off-ramp make 0.5% and 4.6% improvements on the throughput, and 26.8% and 24.1% improvements on the traffic, respectively.

TABLE 5.1 Integrated simulation results between HOV operation and HOT operation under existing traffic demands.

Data output Period: 6:15-9:00 Am		HOV Operation			HOT Operation			Improvement	
		TT[a]	TP[b]	SP[c]	TT	TP	SP	TP	SP
Merging Area 1		48.1	7070	41.2	48.9	7068	40.5	0.0%	-1.5%
HOT Segment 1: Length = 2.8 M	GP+HOV/HOT	339.6	5027	29.5	186.6	5100	53.7	1.4%	82.0%
	GP Lane	364.5	4238	27.3	194.7	2917	51.0	-31.2%	87.2%
	HOV/HOT Lane	166.5	791	59.6	169.2	2184	58.6	176.2%	-1.6%
	On-Ramps	39.6	2737	43.5	26.8	2742	64.2	0.2%	47.6%
	Off-Ramps	112.1	4014	7.0	34.6	4536	22.7	13.0%	224.3%
Merging Area 2		42.1	8750	51.7	40.2	9292	54.1	6.2%	4.7%
HOT Segment 2: Length = 1.3 M	GP+HOV/HOT	132.9	7851	35.2	86.3	8440	54.1	7.5%	54.0%
	GP Lane	139.9	6587	32.6	86.3	5629	52.9	-14.5%	62.2%
	HOV/HOT Lane	78.0	1266	58.6	79.4	2813	57.5	122.2%	-1.7%
	On-Ramps	48.6	1415	38.1	38.3	1421	48.3	0.5%	26.8%
	Off-Ramps	48.7	781	42.6	39.2	817	52.8	4.6%	24.1%
Merging Area 3		62.2	9219	28.6	32.3	9902	55.2	7.4%	92.6%
HOT Segment 3: Length =1.2M	GP+HOV/HOT	125.6	7274	34.2	76.6	7940	56.0	9.2%	63.8%
	GP Lane	129.4	6281	32.2	75.0	5639	55.6	-10.2%	72.6%
	HOV/HOT Lane	71.5	995	58.3	72.3	2302	57.7	131.3%	-1.0%
	On-Ramps	52.3	1381	33.7	30.6	1394	57.5	0.9%	70.7%
	Off-Ramps	45.3	1822	41.5	37.7	1922	49.9	5.5%	20.3%
Merging Area 4		105.8	8595	16.7	33.1	9363	53.2	8.9%	219.4%
HOT Segment 4: Length = 2.4 M	GP+HOV/HOT	246.2	6252	34.6	160.2	6905	53.1	10.5%	53.7%
	GP Lane	258.3	5369	32.6	164.1	4812	51.2	-10.4%	57.4%
	HOV/HOT Lane	142.0	884	59.2	144.1	2095	58.3	136.9%	-1.5%
	On-Ramps	48.7	2467	43.9	42.8	2474	49.9	0.3%	13.7%
	Off-Ramps	39.2	2314	34.1	26.7	2519	50.0	8.9%	46.8%
Merging Area 5		36.9	8638	53.7	42.6	9298	46.5	7.7%	-13.4%
HOT Segment 5: Length = 1.4 M	GP+HOV/HOT	103.4	6507	48.0	93.3	7001	53.2	7.6%	10.9%
	GP Lane	105.7	5115	46.0	94.9	4430	51.2	-13.4%	11.4%
	HOV/HOT Lane	83.1	1393	58.5	84.2	2572	57.7	84.6%	-1.4%
	On-Ramps	18.2	2188	43.8	15.3	2188	52.0	0.0%	18.8%
	Off-Ramps	60.9	2066	39.0	54.2	2241	43.8	8.5%	12.4%

[a] Travel Time (Second), [b] Throughputs, [c] Traffic Speed (Mile Per Hour)

Further simulation tests are conducted by changing traffic demands. Based on the current traffic condition, another four testing scenarios are performed. The simulation results for HOV operations and HOT operations under the 80% and 120% levels of the current traffic demands are summarized in Table 5.2 and Table 5.3, respectively.

Comparing the results shown in Table 5.1 and Table 5.2, we can see that the benefit gained on traffic speed from the HOT operation is less significant in the lower traffic demand condition. For example, the improvement across all three lanes (GP+HOV/HOT) under existing traffic demand on Segment 1 is 82.0%, whereas the improvement across all three lanes (GP+HOV/HOT) under 80% of current traffic demand on Segment 1 is 4.1%. This may due to the fact that, under less congested situation, a lot of SOVs do not find the necessity to pay a toll of using the HOT lane. For example, during the simulation period under the HOV operation with 80% of current traffic demand, the average speed of GP lanes in Segment 1 is 53.3 mph and the average speed of HOV lane is 60.0 mph. The small benefit in speed does not compensate the cost of using a "paid" lane.

We can also see from the same comparison that the benefit gained from HOV to HOT conversion under 120% of current traffic demand is bigger. Under the 120% traffic demand condition, the improvement on the throughput is between 14% and 30% across all five segments, whereas the improvement on the speed is between 15% and 170% for the first four segments. In Table 5.3, the average speed across all three lanes (GP+HOV/HOT) under HOV operation for Segment 2 is only 17.8 mph, whereas the average speed under HOT operation is 45.1 mph.

One less consistent fact is that the average speed across all three lanes (GP+HOV/HOT) under HOV operation for Segment 5 is 46.9 mph, which is higher than that under HOT operation. It is noted that the average speeds in the first four merging areas and individual segments under HOV operation are all less than 20 mph, whereas the average speeds on the segments under HOT operation are all above 30 mph. Moreover, the throughput of all three lanes (GP+HOV/HOT) on Segment 5 under HOV operation is 1,870 (=10,081-8,211) vehicles less than that under HOT operation. This indicates that many SOVs reduced their speed significantly and did not reach Segment 5 at the end of the simulation period.

TABLE 5.2 Integrated simulation results between HOV operation and HOT operation under 80% of the current demands.

Data output Period: 6:15-9:00 Am		HOV Operation			HOT Operation			Improvement	
		TT[a]	TP[b]	SP[c]	TT	TP	SP	TP	SP
Merging Area 1		37.0	5765	53.6	37.8	5765	52.4	0.0%	-2.2%
HOT Segment 1: Length = 2.8 M	GP+HOV/HOT	185.2	4173	54.1	178.0	4151	56.3	-0.5%	4.1%
	GP Lane	186.5	3545	53.3	179.3	2752	55.4	-22.4%	4.0%
	HOV/HOT Lane	165.5	629	60.0	167.8	1400	59.2	122.4%	-1.3%
	On-Ramps	24.6	2209	70.1	22.9	2211	75.4	0.1%	7.5%
	Off-Ramps	33.6	3691	23.3	32.0	3670	24.5	-0.6%	5.0%
Merging Area 2		37.7	7594	57.6	37.6	7575	57.8	-0.2%	0.4%
HOT Segment 2: Length = 1.3 M	GP+HOV/HOT	84.5	6907	55.3	82.3	6884	56.8	-0.3%	2.7%
	GP Lane	83.3	5813	54.8	80.7	5068	56.5	-12.8%	3.2%
	HOV/HOT Lane	77.6	1095	58.9	78.5	1818	58.2	65.9%	-1.2%
	On-Ramps	36.9	1160	50.1	35.3	1163	52.3	0.3%	4.4%
	Off-Ramps	38.8	658	53.4	38.3	657	54.1	-0.1%	1.4%
Merging Area 3		30.9	8102	57.7	30.7	8081	58.0	-0.3%	0.6%
HOT Segment 3: Length =1.2M	GP+HOV/HOT	75.5	6510	56.8	74.8	6492	57.4	-0.3%	1.0%
	GP Lane	73.5	5641	56.6	72.7	5014	57.3	-11.1%	1.2%
	HOV/HOT Lane	70.8	871	58.9	71.7	1479	58.2	69.8%	-1.3%
	On-Ramps	30.5	1129	57.7	30.2	1129	58.3	0.0%	1.0%
	Off-Ramps	36.2	1553	52.0	35.7	1550	52.7	-0.2%	1.4%
Merging Area 4		30.5	7662	57.8	30.4	7646	58.0	-0.2%	0.3%
HOT Segment 4: Length = 2.4 M	GP+HOV/HOT	151.7	5656	56.1	149.0	5639	57.1	-0.3%	1.8%
	GP Lane	150.9	4892	55.7	148.0	4365	56.8	-10.8%	2.0%
	HOV/HOT Lane	141.2	766	59.5	142.8	1275	58.8	66.6%	-1.1%
	On-Ramps	39.2	2004	54.4	38.3	2005	55.7	0.1%	2.3%
	Off-Ramps	25.9	2066	51.5	25.4	2068	52.5	0.1%	2.0%
Merging Area 5		34.6	7598	57.2	34.5	7583	57.2	-0.2%	0.1%
HOT Segment 5: Length = 1.4 M	GP+HOV/HOT	90.6	5722	54.8	88.6	5708	56.0	-0.2%	2.3%
	GP Lane	90.2	4559	54.0	87.8	4068	55.4	-10.8%	2.6%
	HOV/HOT Lane	82.8	1163	58.7	83.3	1642	58.4	41.1%	-0.5%
	On-Ramps	14.3	1773	55.6	14.3	1773	55.9	0.0%	0.6%
	Off-Ramps	50.1	1835	47.4	48.0	1833	49.4	-0.1%	4.3%

[a]Travel Time (Second), [b]Throughputs, [c]Traffic Speed (Mile Per Hour)

TABLE 5.3 Integrated simulation results between HOV operation and HOT operation under 120% of the current demands.

Data output Period: 6:15-9:00 Am		HOV Operation TT[a]	HOV Operation TP[b]	HOV Operation SP[c]	HOT Operation TT	HOT Operation TP	HOT Operation SP	Improvement TP	Improvement SP
Merging Area 1		141.1	6453	14.1	61.8	7521	32.1	16.6%	128.3%
HOT Segment 1: Length = 2.8 M	GP+HOV/HOT	672.6	4386	14.9	246.4	5435	40.7	23.9%	173.0%
	GP Lane	297.2	3040	33.4	296.2	3124	33.5	2.8%	0.4%
	HOV/HOT Lane	169.5	2294	58.5	170.0	2313	58.4	0.8%	-0.2%
	On-Ramps	80.51853	2836.97	21.4	44.8	3074	38.4	8.4%	79.6%
	Off-Ramps	180.1753	3792.727	4.3	99.7	5078	7.9	33.9%	80.8%
Merging Area 2		181.9	7878	11.9	94.1	10133	23.1	28.6%	93.2%
HOT Segment 2: Length = 1.3 M	GP+HOV/HOT	263.2	6942	17.8	103.6	9100	45.1	31.1%	154.1%
	GP Lane	292.0	5772	15.6	109.6	5672	41.6	-1.7%	166.4%
	HOV/HOT Lane	79.1	1174	57.7	84.2	3432	54.3	192.4%	-6.0%
	On-Ramps	90.9	1658	20.4	48.8	1660	37.9	0.1%	86.4%
	Off-Ramps	116.4	747	17.8	39.7	907	52.3	21.5%	193.6%
Merging Area 3		114.7	8568	15.5	53.7	10763	33.2	25.6%	113.7%
HOT Segment 3: Length =1.2M	GP+HOV/HOT	215.3	6651	19.9	134.5	8504	31.9	27.9%	60.1%
	GP Lane	230.7	5727	18.1	155.2	5577	26.8	-2.6%	48.7%
	HOV/HOT Lane	71.5	926	58.3	84.8	2929	49.2	216.2%	-15.7%
	On-Ramps	77.2	1633	22.8	64.5	1634	27.3	0.0%	19.7%
	Off-Ramps	67.0	1800	28.1	44.5	2105	42.2	17.0%	50.4%
Merging Area 4		143.9	8211	12.3	90.5	10081	19.5	22.8%	59.0%
HOT Segment 4: Length = 2.4 M	GP+HOV/HOT	279.3	5852	30.5	243.0	7302	35.0	24.8%	15.0%
	GP Lane	296.8	4984	28.3	292.3	4681	28.8	-6.1%	1.5%
	HOV/HOT Lane	142.0	869	59.2	144.9	2623	58.0	201.7%	-2.0%
	On-Ramps	51.0	2924	41.9	52.8	2925	40.5	0.0%	-3.4%
	Off-Ramps	44.6	2339	29.9	42.4	2727	31.5	16.6%	5.3%
Merging Area 5		36.0	8676	54.9	79.7	10067	24.8	16.0%	-54.8%
HOT Segment 5: Length = 1.4 M	GP+HOV/HOT	105.7	6521	46.9	123.8	7452	40.1	14.3%	-14.6%
	GP Lane	109.2	5015	44.5	138.9	4312	35.0	-14.0%	-21.4%
	HOV/HOT Lane	82.9	1507	58.6	94.5	3142	51.5	108.5%	-12.2%
	On-Ramps	25.5	2593	31.2	40.8	2512	19.5	-3.1%	-37.4%
	Off-Ramps	57.3	2094	41.4	60.4	2424	39.3	15.7%	-5.1%

[a]Travel Time (Second), [b]Throughputs, [c]Traffic Speed (Mile Per Hour)

5.2 Time- of- Day Toll vs. Dynamic Toll

In order to compare the impact from different tolling strategies, toll adjustments based on the time-of-day schedule is also implemented in the COM module using the SR-167 study site as a prototype. Based on the optimized toll rate from the dynamic toll scenarios in 5.1 and the empirical toll rate observation at the SR-167 site, the proposed toll schedule used in the scenarios is as follows:

- 6:00-6:30 am: under lower demand, the toll rate use $1
- 6:30-8:30 am: under higher demand, the toll rate use $2
- 8:30-9:00 am: under lower demand, the toll rate use $1

Three simulation scenarios were designed under time-of-day toll schedule:

a. HOT operation with time of date toll under existing traffic demands
b. HOT operation with time of date toll under 80% of the current traffic demands
c. HOT operation with time of date toll under 120% of the current traffic demands

The simulation results for HOT operation with dynamic toll (Strategy III) and HOT operation with time-of-day toll (Strategy II) under existing traffic demands are summarized in Table 5.4. The last two columns are again the improvement ratio from Strategy II to Strategy III. Based on the results from Table 5.4, the dynamic toll (Strategy III) outperforms time-of-day toll (Strategy II). The throughputs from the two schemes are almost the same. Compared with the Strategy II, Strategy III makes about 1% improvement on the average speed of all three lanes (GP+HOV/HOT) for the first three segments and about 10% improvement on Segments 4 and 5.

For the merging areas, there is not much difference between the two strategies. Strategy III has a higher average speed on Segment 4 across all lanes, whereas Strategy II has a higher average speed on Segment 5 across all lanes. For the on-ramp and off-ramp traffic, Strategy III makes some improvement on average traffic speed in all segments. The improvement of average speed is about 0.5% to 2% for the first three segments, and the improvement increases up to about 5% on Segment 4 and over 10% on Segment 5.

Therefore, the overall performance under Strategy III is better than that of strategy II using the existing traffic demand. This is because Strategy III with a dynamic toll rate is more flexible to adapt itself to the fluctuation of traffic pattern changes. The benefit is expected to be more significant if the traffic demand is much different from normal, e.g. a holiday or sports event.

TABLE 5.4 Integrated simulation results between time of day toll and dynamic toll under existing traffic demands

Data output Period: 6:15-9:00 Am		Time of Day Toll TT[a]	TP[b]	SP[c]	Dynamic Toll TT	TP	SP	Improvement TP	SP
Merging Area 1		48.9	7067	40.6	48.9	7068	40.5	0.0%	0.0%
HOT Segment 1: Length = 2.8 M	GP+HOV/HOT	188.9	5104	53.1	186.6	5100	53.7	-0.1%	1.3%
	GP Lane	197.5	3053	50.3	194.7	2917	51.0	-4.4%	1.4%
	HOV/HOT Lane	169.0	2052	58.7	169.2	2184	58.6	6.5%	-0.1%
	On-Ramps	27.3	2742	63.1	26.8	2742	64.2	0.0%	1.7%
	Off-Ramps	35.2	4546	22.2	34.6	4536	22.7	-0.2%	2.0%
Merging Area 2		40.1	9285	54.2	40.2	9292	54.1	0.1%	-0.1%
HOT Segment 2: Length = 1.3 M	GP+HOV/HOT	87.1	8436	53.6	86.3	8440	54.1	0.1%	0.9%
	GP Lane	87.4	5822	52.2	86.3	5629	52.9	-3.3%	1.3%
	HOV/HOT Lane	79.2	2615	57.7	79.4	2813	57.5	7.6%	-0.2%
	On-Ramps	38.8	1424	47.7	38.3	1421	48.3	-0.2%	1.1%
	Off-Ramps	39.5	815	52.5	39.2	817	52.8	0.2%	0.6%
Merging Area 3		31.9	9902	55.8	32.3	9902	55.2	0.0%	-1.2%
HOT Segment 3: Length =1.2M	GP+HOV/HOT	76.9	7938	55.8	76.6	7940	56.0	0.0%	0.4%
	GP Lane	75.4	5800	55.3	75.0	5639	55.6	-2.8%	0.5%
	HOV/HOT Lane	72.1	2139	57.9	72.3	2302	57.7	7.6%	-0.2%
	On-Ramps	30.7	1395	57.4	30.6	1394	57.5	-0.1%	0.1%
	Off-Ramps	38.0	1924	49.5	37.7	1922	49.9	-0.1%	0.8%
Merging Area 4		34.5	9359	51.1	33.1	9363	53.2	0.0%	4.1%
HOT Segment 4: Length = 2.4 M	GP+HOV/HOT	177.6	6898	47.9	160.2	6905	53.1	0.1%	10.8%
	GP Lane	187.8	4965	44.8	164.1	4812	51.2	-3.1%	14.4%
	HOV/HOT Lane	143.7	1934	58.5	144.1	2095	58.3	8.3%	-0.3%
	On-Ramps	45.0	2474	47.5	42.8	2474	49.9	0.0%	5.1%
	Off-Ramps	28.2	2525	47.3	26.7	2519	50.0	-0.2%	5.7%
Merging Area 5		40.7	9296	48.6	42.6	9298	46.5	0.0%	-4.4%
HOT Segment 5: Length = 1.4 M	GP+HOV/HOT	102.7	7005	48.3	93.3	7001	53.2	-0.1%	10.1%
	GP Lane	108.3	4746	44.9	94.9	4430	51.2	-6.7%	14.1%
	HOV/HOT Lane	84.0	2260	57.9	84.2	2572	57.7	13.8%	-0.3%
	On-Ramps	17.0	2189	46.8	15.3	2188	52.0	0.0%	11.2%
	Off-Ramps	65.7	2243	36.1	54.2	2241	43.8	-0.1%	21.3%

[a]Travel Time (Second), [b]Throughputs, [c]Traffic Speed (Mile Per Hour)

Further simulation tests are conducted by changing traffic demands. The simulation results and comparison between Strategy II and Strategy III under the 80% and 120% levels of the current traffic demands are summarized in Table 5.5 and Table 5.6, respectively.

Comparing Table 5.4 with Table 5.5, no significant difference between the two strategies has been observed. The average speeds of all three lanes (GP+HOV/HOT) are maintained at the same level for the two strategies at Segments 1, 2, and 5. The only difference between two strategies is that under dynamic tolling, more SOVs are shifted to the HOT lane. For example, at Segment 1, there are 38 (2790-2752) less vehicles in GP lanes under the dynamic tolling scenario. However, under this relatively lower demand (80%), this slight difference does not generate significant impact on the network performance.

Comparing Table 5.6 with Table 5.4, the advantages of using dynamic tolling strategy is more prominent under high traffic demand. Under the 120% traffic demand condition, the improvement on the throughput ranges from 0.8% to 2% for these five segments. The improvement on speed is significant at Segments 2 and 3. In Table 5.5, the average speed across all three lanes (GP+HOV/HOT) under Strategy II operation at Segment 2 is only 29.2 mph, while the correspondent average speed under strategy III is 45.1 mph. The average speed at on-ramps and off-ramps under Strategy III also has an over 20% improvement in both Segments 2 and 3. The average speed in Segment 4 under Strategy II is a bit higher than that of Strategy III, which may due to the formation of a bottleneck at the upstream of Segment 4 restricting the vehicles to reach Segment 4.

It is noted from Tables 5.4, 5.5, and 5.6, that the overall network performance under dynamic tolling is better than that under time-of-day tolling with a variety of traffic demand. It further proves that Strategy III is more responsive to different traffic conditions.

TABLE 5.5 Integrated simulation results between time of day toll and dynamic toll under 80% of the current demands.

Data output Period: 6:15-9:00 Am		Time of Day Toll			Dynamic Toll			Improvement	
		TT[a]	TP[b]	SP[c]	TT	TP	SP	TP	SP
Merging Area 1		37.8	5765	52.5	37.8	5765	52.4	0.0%	-0.1%
HOT Segment 1: Length = 2.8 M	GP+HOV/HOT	178.0	4152	56.3	178.0	4151	56.3	0.0%	0.0%
	GP Lane	179.4	2790	55.4	179.3	2752	55.4	-1.4%	0.1%
	HOV/HOT Lane	167.0	1362	59.4	167.8	1400	59.2	2.8%	-0.5%
	On-Ramps	22.9	2218	75.1	22.9	2211	75.4	-0.3%	0.4%
	Off-Ramps	31.9	3679	24.6	32.0	3670	24.5	-0.2%	-0.5%
Merging Area 2		37.5	7572	58.0	37.6	7575	57.8	0.0%	-0.3%
HOT Segment 2: Length = 1.3 M	GP+HOV/HOT	82.3	6880	56.8	82.3	6884	56.8	0.1%	0.0%
	GP Lane	80.7	5107	56.5	80.7	5068	56.5	-0.8%	0.1%
	HOV/HOT Lane	78.5	1774	58.2	78.5	1818	58.2	2.5%	0.0%
	On-Ramps	35.4	1164	52.2	35.3	1163	52.3	-0.1%	0.2%
	Off-Ramps	38.5	656	53.8	38.3	657	54.1	0.2%	0.7%
Merging Area 3		30.7	8082	58.1	30.7	8081	58.0	0.0%	-0.1%
HOT Segment 3: Length =1.2M	GP+HOV/HOT	74.7	6492	57.4	74.8	6492	57.4	0.0%	-0.1%
	GP Lane	72.6	5044	57.4	72.7	5014	57.3	-0.6%	-0.1%
	HOV/HOT Lane	71.7	1449	58.2	71.7	1479	58.2	2.0%	-0.1%
	On-Ramps	30.2	1129	58.4	30.2	1129	58.3	0.0%	-0.1%
	Off-Ramps	35.6	1549	52.8	35.7	1550	52.7	0.0%	-0.1%
Merging Area 4		30.5	7648	57.8	30.4	7646	58.0	0.0%	0.2%
HOT Segment 4: Length = 2.4 M	GP+HOV/HOT	149.2	5642	57.0	149.0	5639	57.1	-0.1%	0.1%
	GP Lane	148.2	4372	56.7	148.0	4365	56.8	-0.2%	0.2%
	HOV/HOT Lane	142.9	1271	58.8	142.8	1275	58.8	0.3%	0.1%
	On-Ramps	38.4	2006	55.6	38.3	2005	55.7	0.0%	0.2%
	Off-Ramps	25.5	2064	52.3	25.4	2068	52.5	0.2%	0.5%
Merging Area 5		34.4	7587	57.5	34.5	7583	57.2	0.0%	-0.5%
HOT Segment 5: Length = 1.4 M	GP+HOV/HOT	88.5	5713	56.0	88.6	5708	56.0	-0.1%	0.0%
	GP Lane	87.8	4137	55.4	87.8	4068	55.4	-1.7%	-0.1%
	HOV/HOT Lane	83.6	1577	58.1	83.3	1642	58.4	4.1%	0.4%
	On-Ramps	14.2	1773	56.2	14.3	1773	55.9	0.0%	-0.6%
	Off-Ramps	47.9	1833	49.5	48.0	1833	49.4	0.0%	-0.2%

[a]Travel Time (Second), [b]Throughputs, [c]Traffic Speed (Mile Per Hour)

TABLE 5.6 Integrated simulation results between time of day toll and dynamic toll under 120% of the current demands.

Data output Period: 6:15-9:00 Am		Time of Day Toll			Dynamic Toll			Improvement	
		TT[a]	TP[b]	SP[c]	TT	TP	SP	TP	SP
Merging Area 1		61.3	7440	32.3	61.8	7521	32.1	1.1%	-0.8%
HOT Segment 1: Length = 2.8 M	GP+HOV/HOT	246.9	5331	40.6	246.4	5435	40.7	2.0%	0.2%
	GP Lane	297.2	3040	33.4	296.2	3124	33.5	2.8%	0.4%
	HOV/HOT Lane	169.5	2294	58.5	170.0	2313	58.4	0.8%	-0.2%
	On-Ramps	44.0	3052	39.1	44.8	3074	38.4	0.7%	-1.8%
	Off-Ramps	94.3	5121	8.3	99.7	5078	7.9	-0.8%	-5.4%
Merging Area 2		73.0	9982	29.8	94.1	10133	23.1	1.5%	-22.5%
HOT Segment 2: Length = 1.3 M	GP+HOV/HOT	159.8	8947	29.2	103.6	9100	45.1	1.7%	54.2%
	GP Lane	186.4	5679	24.5	109.6	5672	41.6	-0.1%	70.1%
	HOV/HOT Lane	106.4	3273	42.9	84.2	3432	54.3	4.9%	26.4%
	On-Ramps	79.2	1656	23.3	48.8	1660	37.9	0.2%	62.5%
	Off-Ramps	51.0	894	40.6	39.7	907	52.3	1.4%	28.6%
Merging Area 3		76.6	10594	23.3	53.7	10763	33.2	1.6%	42.8%
HOT Segment 3: Length =1.2M	GP+HOV/HOT	175.3	8380	24.5	134.5	8504	31.9	1.5%	30.3%
	GP Lane	219.5	5551	19.0	155.2	5577	26.8	0.5%	41.5%
	HOV/HOT Lane	80.5	2832	51.8	84.8	2929	49.2	3.4%	-5.1%
	On-Ramps	77.7	1636	22.7	64.5	1634	27.3	-0.1%	20.5%
	Off-Ramps	57.3	2075	32.8	44.5	2105	42.2	1.4%	28.8%
Merging Area 4		101.3	9962	17.4	90.5	10081	19.5	1.2%	11.9%
HOT Segment 4: Length = 2.4 M	GP+HOV/HOT	241.7	7223	35.2	243.0	7302	35.0	1.1%	-0.5%
	GP Lane	289.0	4682	29.1	292.3	4681	28.8	0.0%	-1.2%
	HOV/HOT Lane	144.4	2544	58.2	144.9	2623	58.0	3.1%	-0.3%
	On-Ramps	51.8	2923	41.2	52.8	2925	40.5	0.1%	-1.9%
	Off-Ramps	42.5	2709	31.4	42.4	2727	31.5	0.7%	0.3%
Merging Area 5		56.6	9969	34.9	79.7	10067	24.8	1.0%	-29.0%
HOT Segment 5: Length = 1.4 M	GP+HOV/HOT	129.2	7390	38.4	123.8	7452	40.1	0.8%	4.4%
	GP Lane	146.2	4522	33.3	138.9	4312	35.0	-4.6%	5.2%
	HOV/HOT Lane	96.0	2870	50.6	94.5	3142	51.5	9.5%	1.6%
	On-Ramps	41.9	2498	19.0	40.8	2512	19.5	0.6%	2.9%
	Off-Ramps	69.6	2418	34.1	60.4	2424	39.3	0.2%	15.3%

[a]Travel Time (Second), [b]Throughputs, [c]Traffic Speed (Mile Per Hour)

5.3 Impacts on the Travel Speed within Different Segments

Sections 5.1 and 5.2 have discussed the impact of different operational strategies on the network-wide performance. This section decomposes the analysis into different time periods and discusses the operational impact within each segment.

5.3.1 Segment 1

Figure 5.1 shows the traffic speed comparisons amongst the three operational strategies for Segment 1 under current traffic demand. It is the average speed across all three lanes and was aggregated every 5-minute. As defined in the earlier section, the three operational strategies are Strategy I (HOV operation), Strategy II (HOT operation with time-of-day toll rate), and Strategy III (HOT operation with dynamic toll). It is shown that Strategy III outperforms the other two in terms of maintaining a satisfying while stable speed (around 50 mph) across the entire time period. Under Strategy I, the average speed begins to fall below 30 mph after 7:20 am.

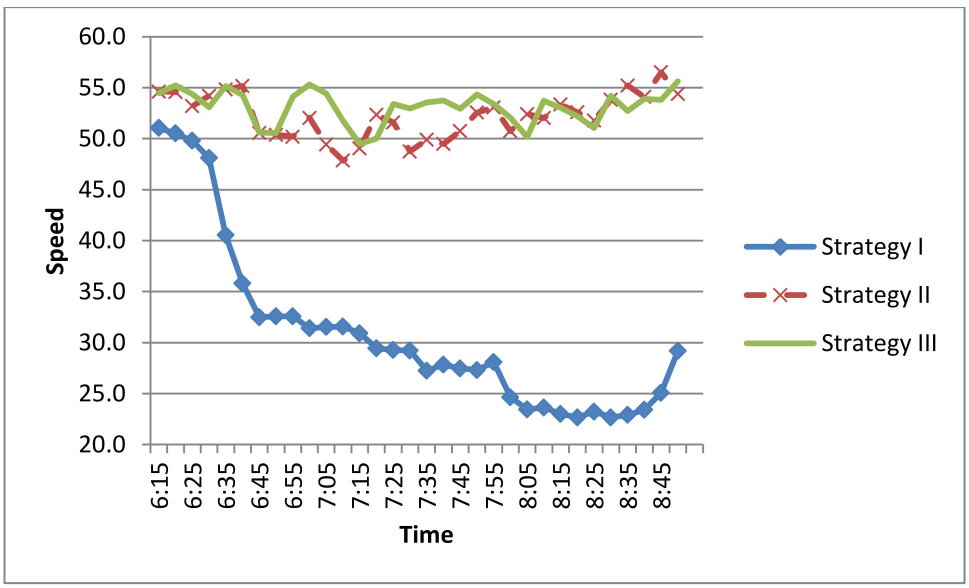

FIGURE 5.1 Traffic speed comparisons among three tolling strategies for Lane Segment 1 under the current demand.

Figure 5.2 shows traffic speed comparisons between the GP and HOV/HOT lanes for Segment 1 under Strategy I and Strategy III with current demand. In Figure 5.2, III-GP represents the average speed of GP lanes under Strategy III; I-GP represents the average speed of GP lanes under Strategy I; III-HOT represents the average speed of the HOT lane under Strategy III; and I-HOV represents the average speed of the HOV lane under Strategy I.

The average speed in the HOV/HOT lane at Segment 1 is stable all the time and all above 57 mph. The average speed of the GP lanes under Strategy III is all above 45 mph, while the average speed of GP lanes under Strategy I falls below to 30 mph after 7:00 am. Therefore, comparing with the HOV operation, dynamic tolling strategy yields a much reliable traffic condition in Segment 1.

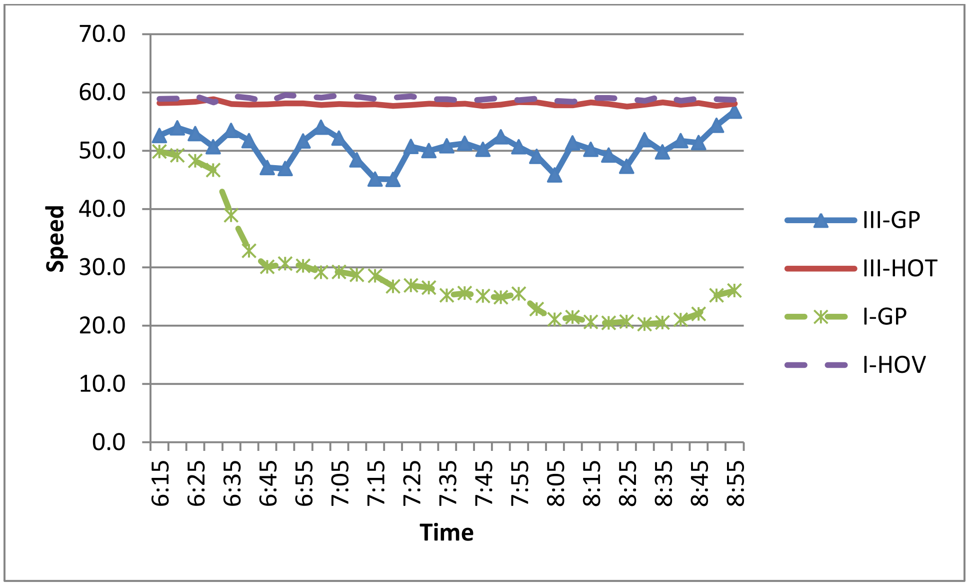

FIGURE 5.2 Traffic speed comparisons between the GP and HOV lanes for Lane Segment 1 under strategy I and strategy III with the current demand.

5.3.2 Segment 2

Figure 5.3 shows the traffic speed comparisons among three tolling strategies for Segment 2 under the current demand. It shows that under Strategy III, the segment 2 performs slightly better than the one under Strategy I. The average speeds for most of the simulation period are above 50 mph. With Strategy I, however, the average speed begins to fall below 40 mph after 6:55 am.

Figure 5.4 shows speed comparison between the GP and HOV/HOT lanes at Segment 2 under Strategy I and Strategy III with the current demand. The average speeds at the HOV/HOT lane in Segment 2 are stable all the time and above 57 mph under both Strategies I and III. The average speed of the GP lanes under Strategy III is all above 46 mph, while the average speed of GP lanes under Strategy I falls below to 40 mph after 6:50 am. Therefore, comparing with the HOV operation, dynamic tolling strategy proves to be more effective in maintaining a better performance for both GP and HOT lanes.

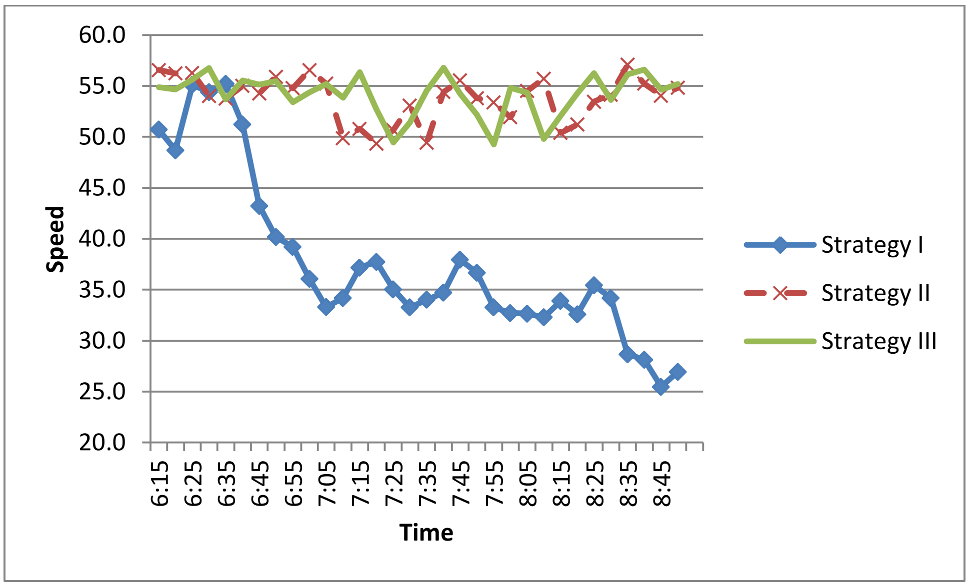

FIGURE 5.3 Traffic speed comparisons among three tolling strategies for Lane Segment 2 under the current demand.

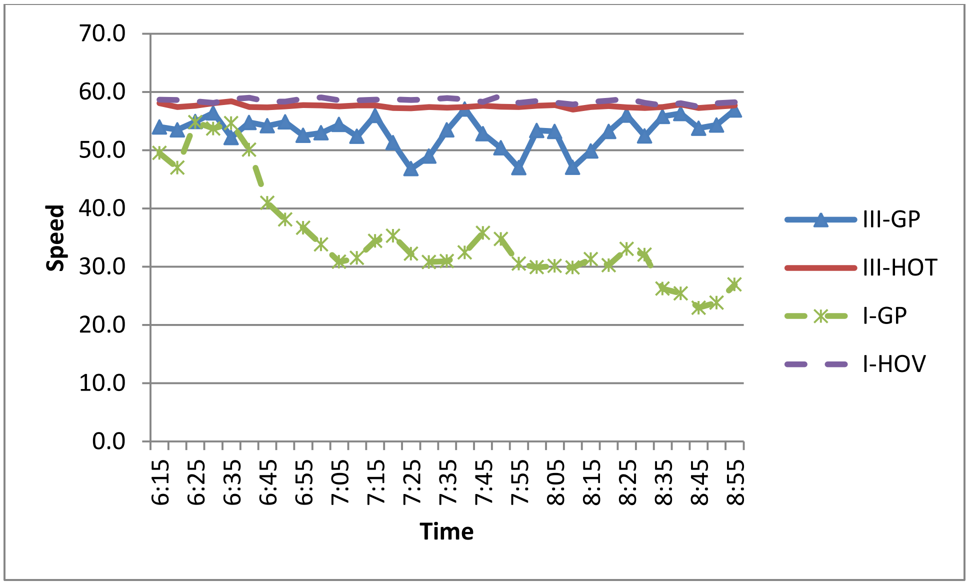

FIGURE 5.4 Traffic speed comparisons between the GP and HOV lanes for Lane Segment 2 under strategy I and strategy III with the current demand.

5.3.3 Segment 3

Figure 5.5 shows the speed (across all lanes) comparison among three tolling strategies for Segment 3 under current demand. The average speed for most of the time is above 54 mph under both Strategies II and III. With Strategy I, the average speed significantly decreases after 7:45 am and begins to fall below 30 mph after 8:00 am.

Figure 5.6 shows speed comparison between the GP and HOV lanes for Segment 3 under Strategy I and Strategy III with the current demand. The average speed from the HOV/HOT lane is stable all the time and is all above 56 mph under both Strategies I and III.

The average speed of the GP lanes under Strategy III is all above 53 mph, whereas the average speed of GP lanes under Strategy I falls below to 30 mph after 8:00 am. Again, dynamic tolling strategy outperforms the HOV operation for Segment 3.

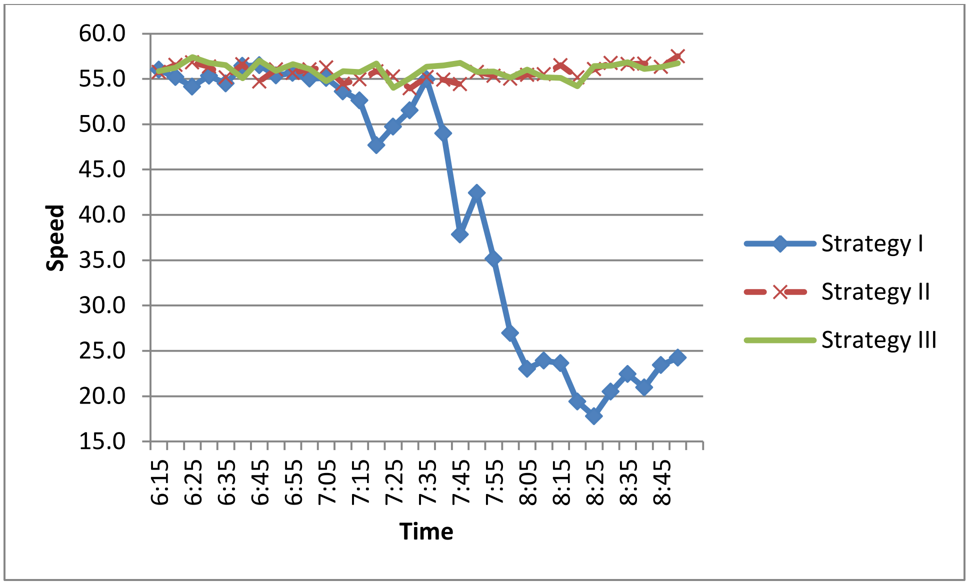

FIGURE 5.5 Speed comparison among three operational strategies for Segment 3 under the current demand.

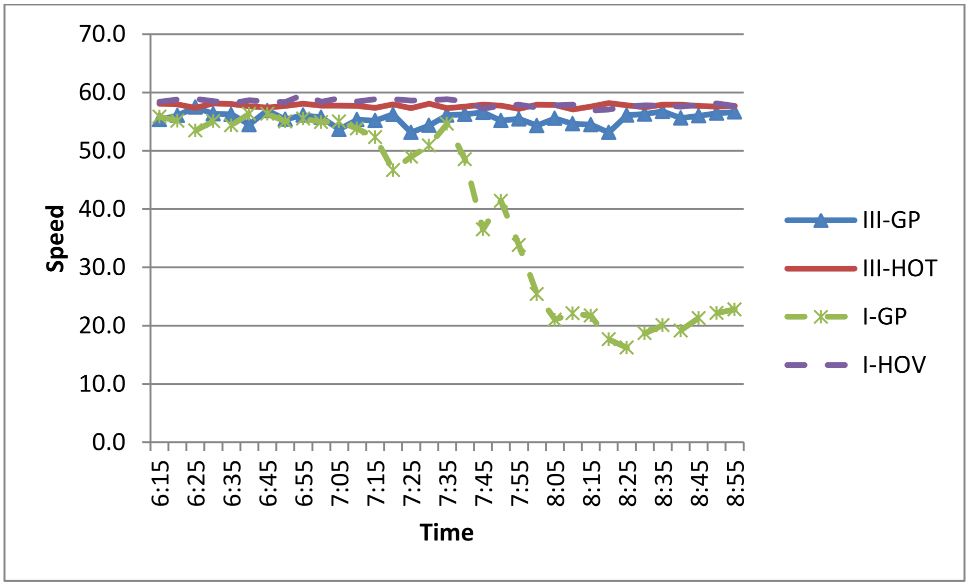

FIGURE 5.6 Speed comparison between the GP and HOV/HOT lanes for Segment 3 under strategy I and strategy III with the current demand.

5.3.4 Segment 4

Figure 5.7 shows the speed comparison among three operational strategies for Segment 4 under the current demand. The speed in Figure 5.7 is the average speed of across all three lanes and aggregated every 5 minute. It is noted that Strategy III performs better than Strategy II, especially during the time period 7:30-8:20 am. For example, the average speed under Strategy II during time period 7:40-8:10 am is about 41 mph whereas it is about 53 mph under Strategy III. Under strategy I, the average speed begins to fall below 40 mph after 6:55 am.

Figure 5.8 shows traffic speed comparison between the GP and HOV/HOT lanes for Segment 4 under Strategy I and Strategy III with the current demand. The average speeds in the HOV/HOT are stable all the time and all above 57 mph in both Strategies I and III. The average speed of the GP lanes under Strategy III is all above 45 mph, whereas the average speed of GP lanes under strategy I falls below to 40 mph after 6:55 am.

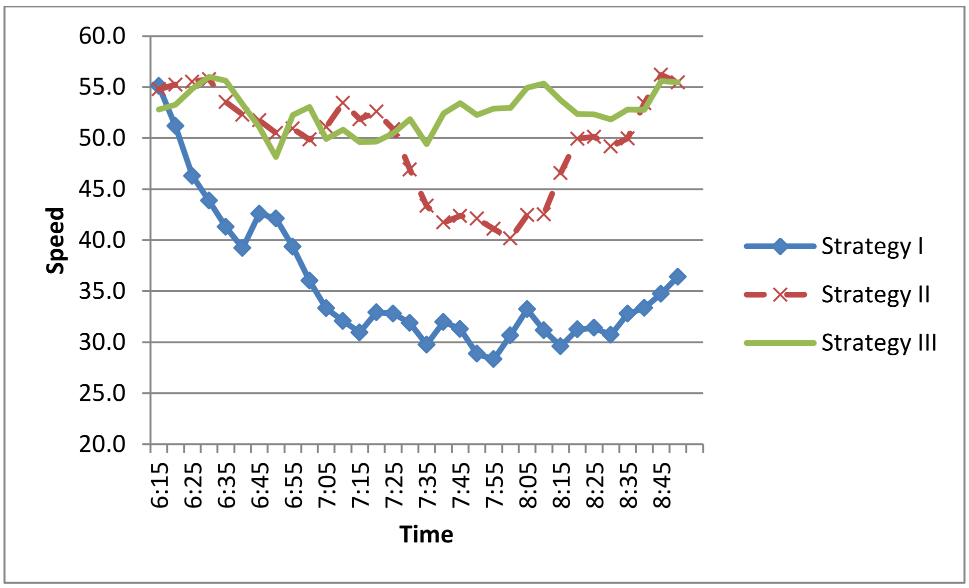

FIGURE 5.7 Traffic speed comparisons among three tolling strategies for Segment 4 under the current demand.

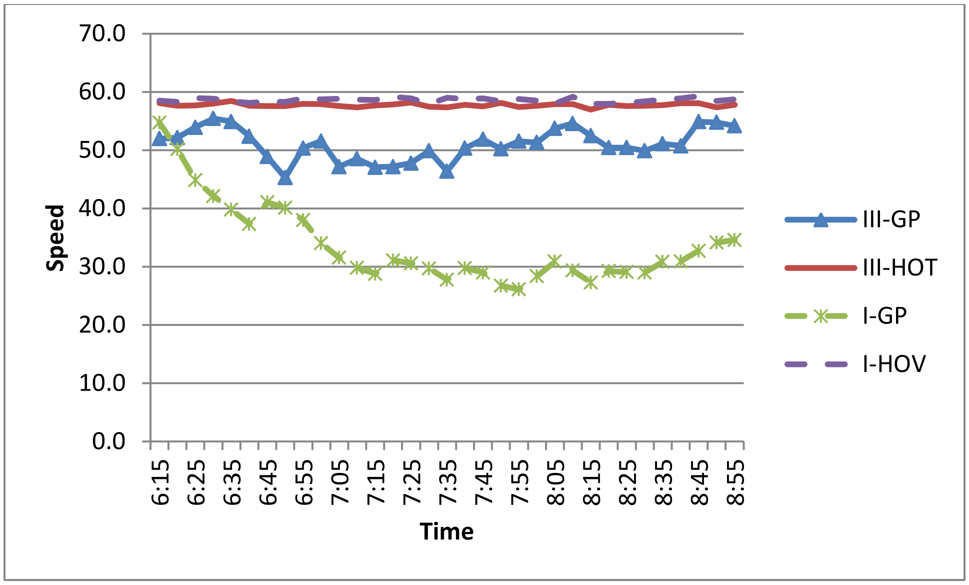

FIGURE 5.8 Traffic speed comparisons between the GP and HOV lanes for Segment 4 under strategy I and strategy III with the current demand.

5.3.5 Segment 5

Figure 5.9 shows the speed comparison among three operational strategies for Segment 5 under the current demand. The speed in Figure 5.9 is the average speed of across all three lanes. It can be seen from Figure 5.9 that Strategy III performs better than Strategy II, especially after 7:50 am. For example, the average speed under Strategy II during time period 8:10-8:20 am is about 43 mph while it is about 55 mph under Strategy III. The performance in Segment 5 under Strategy I is not as bad as the previous segments due to the fact that the congestion in the upstream delayed the vehicles' arrival Segment 5 during the simulation period.

Figure 5.10 shows speed comparison between the GP and HOV/HOT lanes for Segment 5 under Strategy I and Strategy III with the current demand. The average speeds of the HOV/HOT lane are stable all the time and all above 57 mph in both Strategies I and III. The improvement on the GP lane under strategy III is not as significant as in the previous segments since not all the vehicles are able to reach Segment 5 at the end of the simulation under Strategy I. The average speed of the GP lanes under Strategy III is all above 43.9 mph, whereas the average speed of GP lanes under Strategy I falls below to 40 mph in during the time periods of 7:30-7:35 am and 7:45-7:50 am.

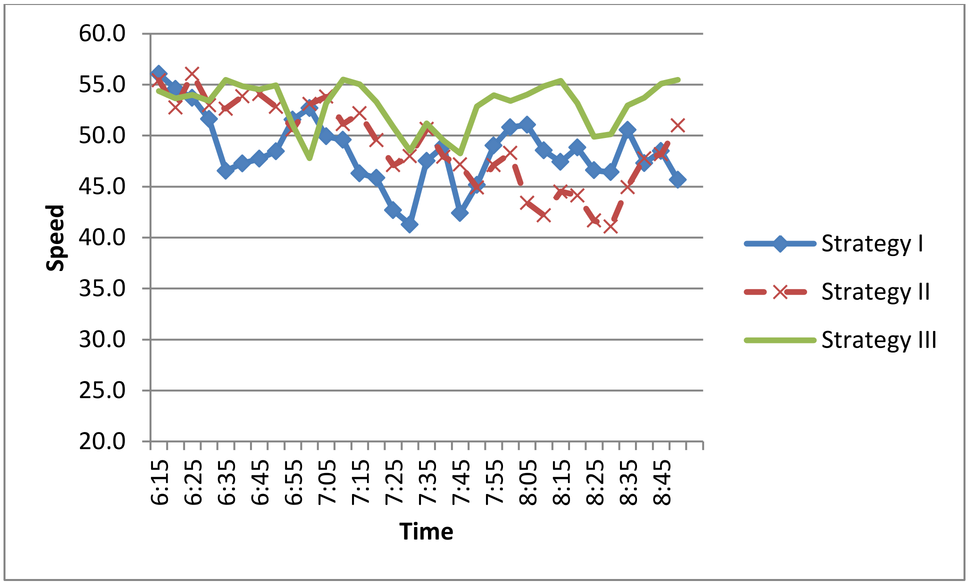

FIGURE 5.9 Traffic speed comparisons among three tolling strategies for Segment 5 under the current demand.

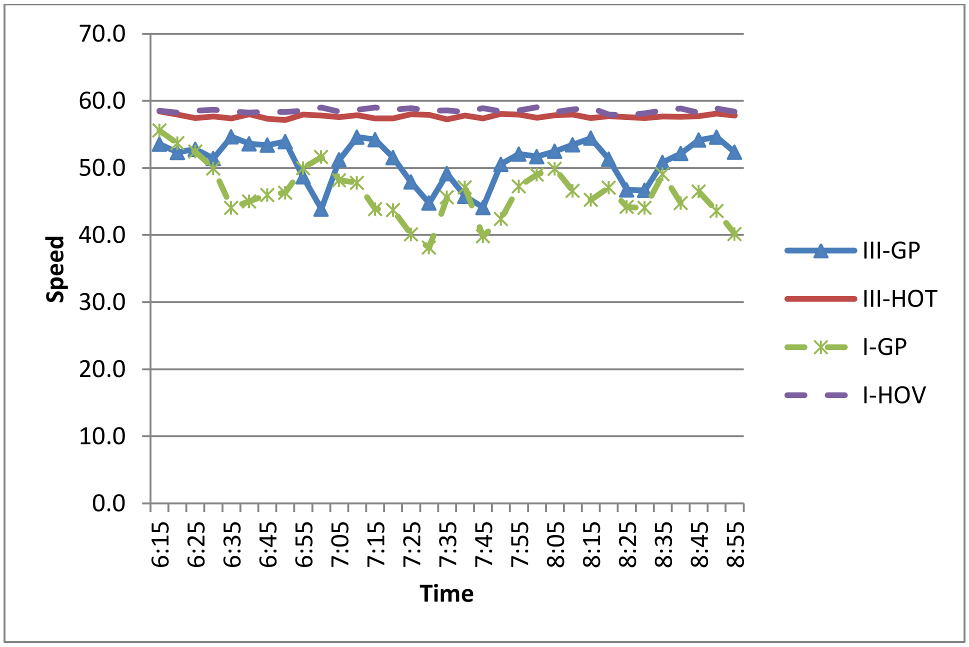

FIGURE 5.10 Traffic speed comparisons between the GP and HOV lanes for Segment 5 under strategy I and strategy III with the current demand.

5.4 Impacts on the Overall Network Performances

Traffic emission is one of the main sources of air pollution. Studies have found that vehicles emit more pollutants under congested traffic conditions. Congestion pricing helps to reduce air pollution through managing the traffic demand and improving traffic network efficiency if the management implements properly. NOx is the major component of the traffic emission. Therefore, during the simulation, the emission of NOx is also considered as a performance measure towards the efficiency of operational strategies.

Tables 5.7, 5.8, and 5.9 list the overall network performances under different management strategies with 80%, 100%, and 120% of existing traffic demand. Again, Strategy I represents HOV operation; Strategy II represents HOT operation with time-of-day tolling schedule; and Strategy III represents HOT operation with dynamic toll. Three improvement ratios are calculated: *a* represents the improvement ratio from Strategy I to Strategy II; *b* represents the improvement ratio from Strategy I to Strategy III; *c* represents the improvement ratio from Strategy II to Strategy III.

It is noted from the result that Strategy III performs best amongst the three under a variety of demand in term of the overall network performance. As the demand increases, the reduction in emission and improvement in travel speed (from Strategy I or II to Strategy III) demonstrate a positive trend. Use the emission NOx as an example, the improvement ratio *c*, from Strategy I to Strategy III, is 0.46% under 80% demand, 1.92% under exiting demand, and 3.96% under 120% demand.

Comparing with the other two strategies, the average speed on HOT and GP lanes under Strategy III has some improvement in all three scenarios. The reason that the HOT lane has a higher speed under Strategy III than that under Strategy I can probably ascribe to the fact that the congestion formed in GP lanes and merging areas under Strategy I has a negative impact on the HOV lane as well.

TABLE 5.7 Network performances among different management strategies under 80% of the current demands.

	Management Strategies			Improvement		
	I	II	III	a	b	c
Emissions NOx [kg]	867.8	857.0	853.1	1.24%	1.69%	0.46%
Average speed [mph]	56.16	56.82	56.85	1.18%	1.23%	0.05%
Average delay time per vehicle [s]	25.65	20.56	20.42	19.84%	20.38%	0.67%
Average number of stops per vehicles	0.33	0.22	0.23	33.45%	31.64%	-2.73%
Average speed for SOV [mph]	55.56	56.43	56.45	1.58%	1.61%	0.03%
Average delay time per vehicle HOV [s]	30.67	23.90	23.65	22.08%	22.89%	1.03%
Average speed for HOV [mph]	57.65	57.61	57.66	-0.07%	0.02%	0.10%
Average delay time per vehicle for HOV [s]	13.06	12.99	12.98	0.56%	0.68%	0.12%

TABLE 5.8 Network performances among different management strategies under the current demands.

	Management Strategies			Improvement		
	I	II	III	a	b	c
Emissions NOx [kg]	1354.0	1138.9	1117.1	15.88%	17.50%	1.92%
Average speed [mph]	40.57	52.18	53.14	28.63%	31.00%	1.84%
Average delay time per vehicle [s]	185.02	58.26	49.86	68.51%	73.05%	14.42%
Average number of stops per vehicles	9.09	1.33	1.00	85.35%	89.02%	25.06%
Average speed for SOV [mph]	37.68	50.92	52.14	35.11%	38.35%	2.40%
Average delay time per vehicle HOV [s]	231.16	70.46	59.28	69.52%	74.36%	15.87%
Average speed for HOV [mph]	49.26	55.00	55.09	11.66%	11.84%	0.16%
Average delay time per vehicle for HOV [s]	75.21	31.09	30.22	58.66%	59.82%	2.81%

TABLE 5.9 Network performances among different management strategies under 120% of the current demands.

	Management Strategies			Improvement		
	I	II	III	a	b	c
Emissions NOx [kg]	2294.1	1975.3	1896.9	13.90%	17.31%	3.96%
Average speed [mph]	24.64	32.59	34.20	32.30%	38.81%	4.92%
Average delay time per vehicle [s]	504.70	317.19	286.56	37.15%	43.22%	9.65%
Average number of stops per vehicles	36.26	13.96	11.58	61.50%	68.06%	17.05%
Average speed for SOV [mph]	21.11	29.84	31.66	41.33%	49.94%	6.09%
Average delay time per vehicle HOV [s]	641.44	383.74	342.51	40.18%	46.60%	10.74%
Average speed for HOV [mph]	35.34	38.56	38.98	9.10%	10.28%	1.08%
Average delay time per vehicle for HOV [s]	227.68	189.14	184.84	16.93%	18.82%	2.28%

CHAPTER 6 SR-520 EVERGREEN POINT BRIDGE TESTBED

After tolling has been implemented on the SR-520 Evergreen Point Bridge, travelers' behavior might change. Some people may adjust their departure time for a discount toll rate; some people may choose a different destination to avoid the toll. Considering these behavior changes, two scenarios are designed in this research project:

- Scenario 1: traffic demand is assumed to be unchanged before and after the toll implementation. In order to identify the tolling impact on the freeway travel, four different toll rates are considered in this scenario: $0, $1, $3.5, and $7. $0 is the base case indicates that the toll is not implemented; $3.5 is the rate proposed by WSDOT; $1 and $7 represent lower and higher reference rates, separately.
- Scenario 2: there is a 5% reduction in traffic demand crossing the Lake Washington during morning peak hour after the toll implementation. The reduced demand may be attributable to the travelers that start carpooling with others or shift their departure time to avoid the higher toll. The 5% assumption is based on the updated statistics from WSDOT Toll Division (Craig et al., 2012).

In this testbed, Car2X module in VISSIM is used in the simulation. The morning peak is used as an example to simulate the toll rate impact on the highway travel. Traffic dynamics from the east side of Lake Washington to the west side of Lake Washington is the focus in this research. The evening peak can be evaluated in a similar fashion. Morning peak traffic demands of the central freeway framework of Puget Sound area encompassing SR-520, I-5, I-90, and SR-405 from 7:30am to 8:30 am period are collected.

The simulation output used for simulation network performance evaluation was extracted from 8:00 am to eliminate the initial warm-up period. To accommodate the randomness of simulation results and enhance simulation models' credibility, each simulation scenario was conducted under multiple random seeds. Two MOEs, traffic speed (space-mean speed) and throughput, are used as the performance indicators. These two indicators are compared amongst different toll rate under scenario 1 in Sections 6.1 and Section 6.2. The impacts on the overall network from different toll rates under scenario 1 are described in Section 6.3. The results from scenario 2 are discussed in Section 6.4.

6.1 Impacts on the Travel Speed within Different Segments

During the morning peak period, the traffic demand from the east side of Lake Washington to the west side of Lake Washington is higher than the reversed direction. Therefore the WB of SR-520 is the focus in this scenario. To analyze the toll impact, six segments are evaluated (as shown in Figure 6.1): SR-520 WB, I-90 WB, I-5 SB, I-5 NB, I-405 SB and I-405 NB.

Table 6.1 shows the lengths for these six segments and Table 6.2 shows the simulation results for the average speed at different segments under different toll rates. Based on Table 6.2, it is noted that:

- With a higher toll rate in SR-520, less people would use SR-520 and thus an increase in travel speed on SR-520 is observed.
- The travel speed on I-90 decreases as the SR-520 study site's toll rate increase. This is because some of the vehicles switched their routes from the SR-520 to I-90.
- I-5 traffic condition was not affected much as the toll rate changes. This may due to the fact that the volume change of SR 520 is not significant comparing with its own throughput that I-5 carries on a daily basis.
- The situation on I-405 is similar to I-5. There is not much significant variation in speed as the toll rate changes.

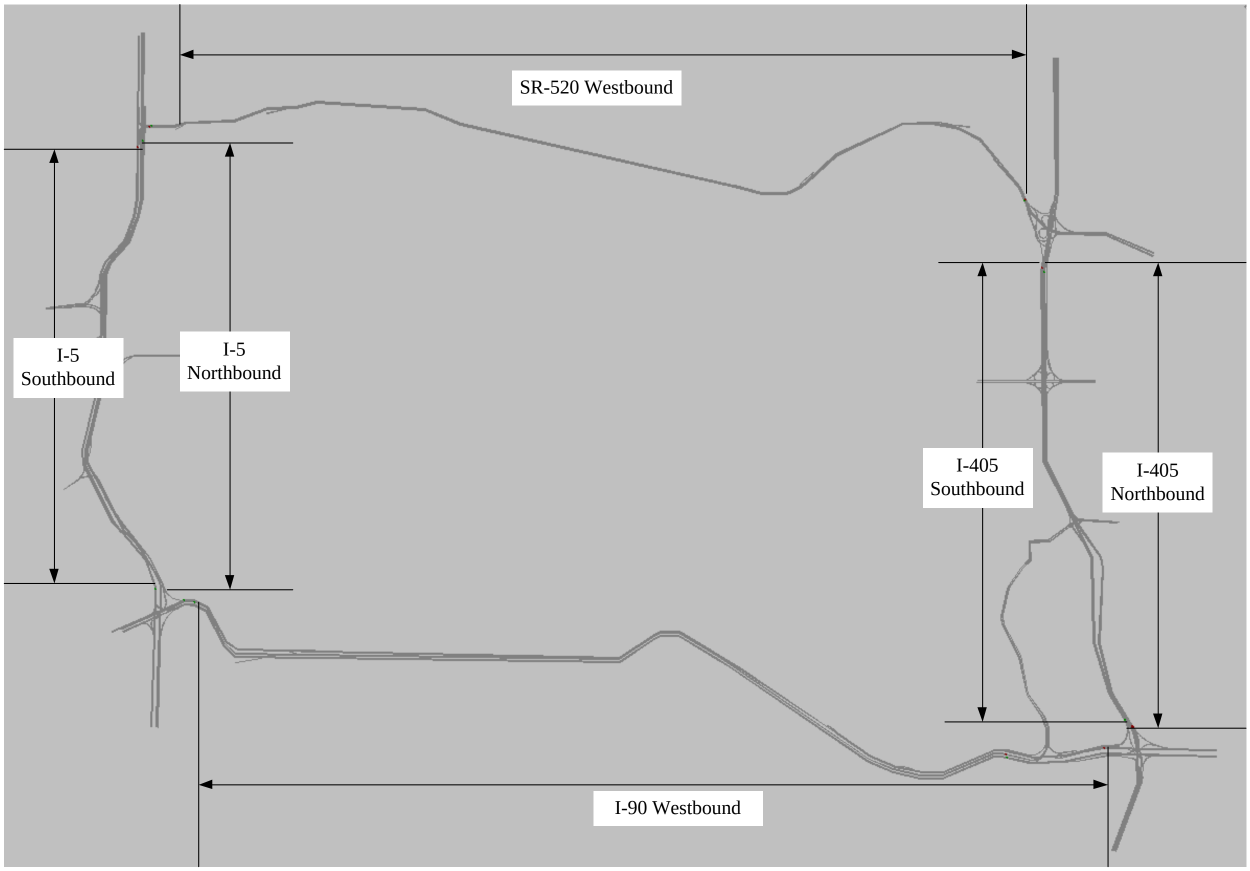

FIGURE 6.1 Six evaluated segments in the simulation network.

TABLE 6.1 Segment lengths of the six evaluated segments

Segment	SR-520 Westbound	I-90 Westbound	I-5 Southbound	I-5 Northbound	I-405 Southbound	I-405 Northbound
Length (mile)	6.42	6.79	3.22	3.43	3.19	3.24

TABLE 6.2 Average speeds (mph) within different segments under different toll rate.

Toll Rate	SR-520 Westbound	I-90 Westbound	I-5 Southbound	I-5 Northbound	I-405 Southbound	I-405 Northbound
$0	28.6	48.0	46.9	43.9	57.4	45.8
$1	31.4	46.3	46.4	43.5	56.8	46.1
$3.5	33.7	46.5	43.8	43.2	57.6	48.2
$7	35.6	45.8	47.7	43.4	57.1	46.2

6.2 Impacts on the Throughput

Table 6.3 shows the total throughput for the six segments during the simulation period. It can be found from Table 6.3 that even though the travel speeds on the SR-520 and I-90 are affected by toll rate, the throughputs of the freeways do not have a significant change except for I-405 Southbound. This might due to the fact that during the peak period, those freeways are already operating at capacity. For I-405 SB, however, the corridor is not reaching capacity as the average speed is still above 55 mph. And as the toll rate goes high, more vehicles would switch from SR-520 to I-90, which results in a demand increase on I405 SB.

In summary, in scenario 1, the toll rate has an impact on the segment throughputs but not significant. This is because in scenario 1, the total demand keeps the same with different toll rate. During the peak hour, there is not much room for vehicles switch their route from SR-520 to I-90 due to the capacity limit on I-90. If the local streets are included in the network or people switch their travel to other time period, like scenario 2, the impact is expected to be bigger. Further research is necessary in the future.

TABLE 6.3 Total throughputs within the six evaluated segments during the simulation time period.

Toll Rate	SR-520 Westbound	I-90 Westbound	I-5 Southbound	I-5 Northbound	I-405 Southbound	I-405 Northbound
$0	3429	5012	6770	4895	4749	5803
$1	3443	4956	6639	4886	4707	5879
$3.5	3441	5023	6704	4881	4744	5839
$7	3438	5013	6676	4885	4801	5870

6.3 Impacts on the Overall Network Performances

Vehicles would generate more emission and consume more fuel during traffic congestion. Therefore, the NOx emission and fuel consumption are also considered as the indicators for evaluating network performances. Table 6.4 lists four indicators, average delay, average speed, emissions NOx and fuel consumption, for evaluating the network performance for different toll rates. It is found that the network performance improves when the toll rate change from $0 to $7 in scenario 1. For example, when he toll rate change from $0 to $7, the average speed in the network increases from 47.3 mph to 48.1mph and the

NOx emission decreases from 1573.5kg to 1553.1kg. However, it is still not conclusive whether the network performance would have further improvement if the toll rate is higher than $7 as the traffic from I-405 to I-90 may block I-405 when there is excessive traffic trying to get into I-90. Moreover, traffic from SR-520 WB to I-405 SB can also block SR-520 as well when there are too many vehicles switch their route from SR-520 to I-90.

TABLE 6.4 Network performances among different toll rates during the simulation time period.

	$0	$1	$3.5	$7
Average delay time per vehicle [s]	77.3	74.0	74.0	74.2
Average speed [mph]	47.3	47.7	48.1	48.1
Emission NOx [kg]	1573.5	1566.7	1553.9	1553.1
Fuel Consumption [kg]	983.5	979.2	971.2	970.7

6.4 Impacts on the Travel Speed under Scenario 2

Sections 6.1-6.3 discussed the toll impact under scenario 1. This section considers the traffic demand variation affected by toll implementation. Under scenario 2, we assume that there is a 5% reduction in traffic demand on SR-520 during the peak hour after toll implement (Craig et al., 2012).

Tables 6.5 and 6.6 show the average speed and total throughputs at different segments under the two scenarios, respectively. From Tables 6.5 and 6.6, it can be found that:

- Comparing with scenario 1, scenario 2 gets much improvement on the SR-520, the average speed increases from 33.7mph to 55.2mph. The throughput also decreased from 3441 to 3194. This indicates that after the reduction been made, the volume pass through the SR-520 Bridge is still close to its original volume, which is only decrease by 7%, however, the speed has an very huge improvement.
- For I-90, although the through put remains a similar amount among different scenarios and toll rate, but a clear trend can be generated that the speed decreases as toll gets higher. That might because the volume on I-90 is already close to its capacity during the peak hour. Even though there is more vehicles choose I-90 to avoid the tolling on SR-520, the throughput will not change much when it is already reach the capacity. But we can tell there is more vehicles using I-90 since the travel speed decrease after the tolling.

TABLE 6.5 Average speeds (mph) within different segments under different scenario.

Conditions	SR-520 Westbound	I-90 Westbound	I-5 Southbound	I-5 Northbound	I-405 Southbound	I-405 Northbound
No Toll	28.6	48.0	46.9	43.9	57.4	45.8
Scenario 1 (toll= $3.5)	33.7	46.5	43.8	43.2	57.6	48.2
Scenario 2 (toll= $3.5)	55.2	46.7	47.9	43.0	57.8	46.7

TABLE 6.6 Total throughputs within different segments under different scenario segments during the simulation time period.

Conditions	SR-520 Westbound	I-90 Westbound	I-5 Southbound	I-5 Northbound	I-405 Southbound	I-405 Northbound
No Toll	3429	5012	6770	4895	4749	5803
Scenario 1 (toll= $3.5)	3441	5023	6704	4881	4744	5839
Scenario 2 (toll= $3.5)	3194	4973	6729	4858	4665	5807

6.5 Comparing with loop data

The loop detectors in the study area can provide some information for the traffic condition of SR-520 and I-90. The volume and speed collected by the dual loop are stored in the Digital Roadway Interactive Visualization and Evaluation Network (Drive Net) developed by the Smart Transportation Applications and Research Laboratory (STAR Lab) of the University of Washington. To test the simulation results, the morning peak hour data (8:00 AM to 8:30 AM) during the weekday (Monday to Thursday) before the toll (March7 to 10, 2011) and after the toll (March 12 to 15, 2012) are derived from Drive Net for validation.

As shown in Table 6.7, the results of our simulation in scenario 2 are close to the results from the loop data. For the results from the loop data, the volume of SR-520 deceased and the speed increased, which are similar to the results of the simulation. However, the change from the results of loop data is a little bigger than what we get form the simulation testbed. This might because many people do not want to pay the toll, even if the value of time saved exceeds the value of toll rate. For I-90, the change in speed is also a little bigger than that in the simulation, but the volume doesn’t change much. These implies that the volume in I-90 is very close to its capacity during peak hour, and extra volume induced to this route would only cause a drop in speed rather than an increase in volume.

TABLE 6.7 major test bed and real world data compare

Condition	SR520 W Before Tolling	SR520 W After Tolling	I90 W Before Tolling	I90 W After Tolling
Speed(testbed)	28.6	55.2	48.0	46.5
Speed (loop data)	34.1	55.9	47.6	42.4
Volume (testBed)	3429	3194	5012	4973
Volume (loop data)	2918	2584	4965	5037

CHAPTER 7 SIMULATION MODEL CALIBRATION AND OUTPUT ANALYSIS

As mentioned in the literature review, simulation model calibration and output data analysis are the key issues for the simulation study. The SR-167 HOT Lane testbed is used as an example in this chapter. Details of the research team's simulation work on the SR-167 HOT Lane has been published in Zhang et al. (2008 and 2009).

7.1 Simulation Model Calibration

The simulation model for the SR-167 study site was previously developed by Zhang et al. (2009). Based on the base-year traffic planning survey data, SOV, HOV, and truck OD matrices are estimated and inputted to the simulation model. Through multiple iterations of traffic assignment, these traffic demands are allocated to the whole study area of SR-167 and the assignment equilibrium is achieved. To check the fidelity of this simulation model, virtual loop sensors are placed in the simulation model according to their real positions on ramps and arterial roadways. Traffic counts and speeds are collected from these virtual loop detectors and compared to the reference data. If they are significantly different, then trip attraction and production in the OD matrices are rebalanced so that the difference can be reduced. These steps are iterated until the volume difference is reasonably small (less than 10%).

Annual average traffic volumes and speeds are utilized to calibrate the driving behavior parameters. In VISSIM, traffic flow is modeled as a discrete and stochastic process, in which each driver-vehicle-unit is treated as a single entity. The freeway car following logic uses the Wiedemann 99 Model (PTV 2007; Wiedemann 1991) and involves ten parameters, including standstill distance, headway time, etc. In this study, three major parameters: standstill distance, headway time, and minimum lane changing headway, are adjusted according to the observed field headway data. Also, other parameters, such as the look-back distance, etc. are modified individually for weaving areas. A detailed driving behavior calibration procedure for freeway operations can be found in Gabriel's research (2004). After tuning up these parameters, the simulation model is iteratively executed until traffic assignment is equilibrated in the network. Based on the comparisons between the simulation results and the corresponding reference data, such calibration processes are repeated. Once the difference is small enough, the model is considered reasonably calibrated and is ready for HOT lane simulations.

To verify the overall reliability of the calibrated simulation model, five important locations on the SR-167 corridor and two locations on the I-450 interchange bridge are chosen as check points. Simulated traffic volumes and speeds are compared with ground-truth data at these check points. For example, Figure 7.1 and Figure 7.2 provide visual comparisons of traffic volumes and speeds at the location of SR-167 & 277th St.

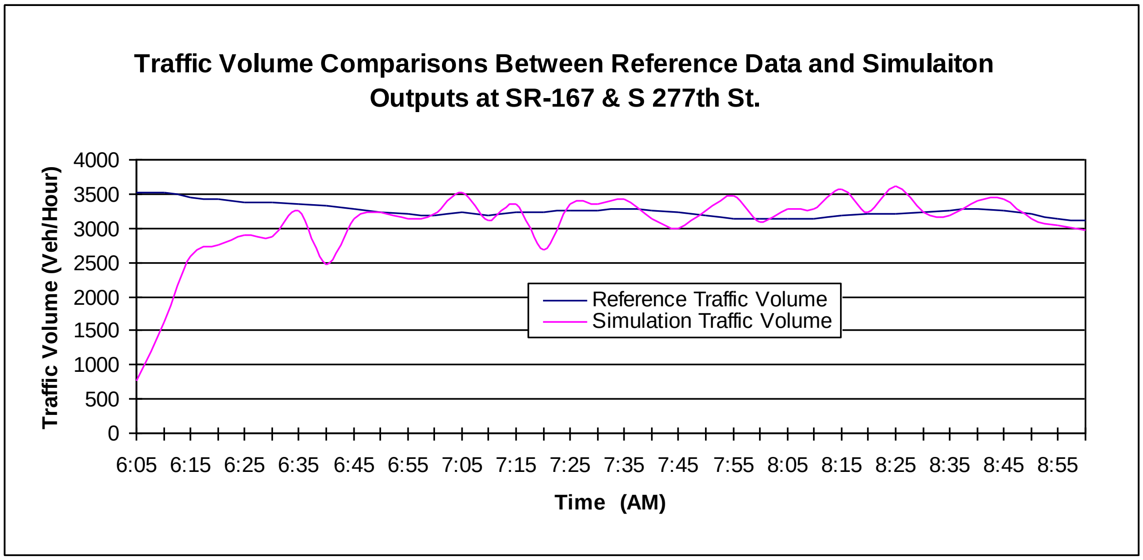

FIGURE 7.1 Traffic volume comparisons between reference data and simulation outputs at the location of SR-167 & 277th St. (Source: Zhang et al., 2009)

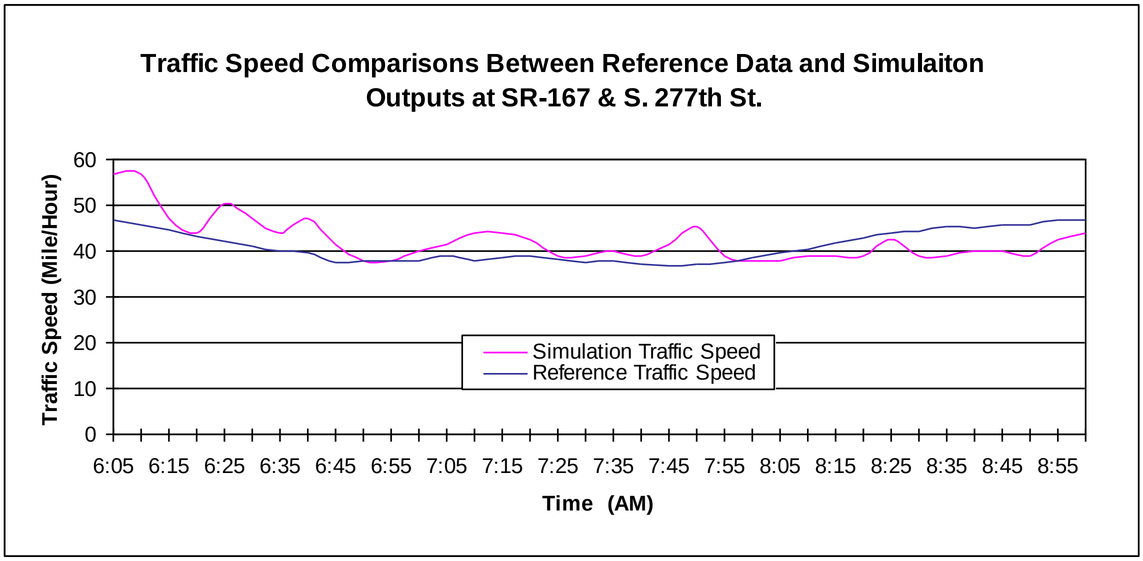

FIGURE 7.2 Traffic speed comparisons between reference data and simulation outputs at the location of SR-167 & 277th St. (Source: Zhang et al., 2009)

We can see that traffic volumes and speeds produced by the simulation model slightly fluctuate around the corresponding ground-truth annual average values. Considering the randomness of simulation outputs, such minor discrepancies are acceptable. Note that within the three-hour simulation period from 6:00am to 9:00am, traffic takes some time to gradually flow into the network and become stable. Also, vehicles generated near the end of the simulation period may not be able to complete their journey. Therefore, to avoid possible biased results, our analysis concentrates on one representative hour from 7:30am-8:30am to screen out unfavorable disturbances. Table 7.1 shows descriptive statistics for both simulation outputs and their corresponding observed annual average values. Although simulation outputs have a bigger variation than the annual average ground-truth values, their mean values are reasonably close for both volumes and speeds. Based on both volume and speed comparisons at several vital locations, we believe that the overall simulation outputs are reasonably consistent with the reference data. Therefore, we conclude that the model is well calibrated and can produce reliable analyses and results.

TABLE 7.1 Descriptive statistics for both simulation outputs and their corresponding annual average values。

Time: 7:30am-8:30am		Simulation Outputs				Annual Average Traffic Data			
		Volumea		Speedb		Volume		Speed	
		Mean	Stdc	Mean	Std	Mean	Std	Mean	Std
SR-167	15th St. NW	3266	196.62	42.27	8.35	3224	61.90	39.75	3.25
	S. 277th St.	3303	177.73	39.67	2.75	3200	50.57	39.84	2.13
	SR 516/Kent-Des Moines Rd.	3381	127.11	47.41	3.64	3379	108.67	45.42	0.43
	S. 212th St.	3155	144.79	43.25	7.25	3128	75.85	43.13	1.00
	SW 43rd ST.	2964	102.65	45.83	9.84	2985	70.12	42.46	1.52
I-405	SB Milepost 1.5	3342	179.84	42.02	0.87	3571	32.83	38.83	0.51
	NB Milepost 2.5	1700	232.81	56.44	3.07	1535	35.78	56.74	0.71

[a] Vehicle Per Hour, [b] Mile Per Hour, [c] Standard Deviation

Source: Zhang et al. (2009)

7.2 Simulation Output Analysis

7.2.1 Interval Estimates from Multiple Simulation Runs

For the bootstrap analysis of multiple random seed simulation, the Dynamic Toll scenario with current demand (100%) is used to demonstrate the statistical analysis procedure. In total, 37 random seeds were run for this scenario to accommodate different traffic inflow arrival patterns. Segment 1 GP lanes' speed is chosen for performing the speed interval estimates. The speed data are aggregated every 15-minute, and started to be collected from 900 simulation seconds to eliminate the simulation initialization period impact. Figure 7.3 shows the speed profile from the Segment 1 GP lane for three consecutive 15-min time intervals under various random seeds. It is noted that the simulation output under different random seeds could vary quite significantly. Therefore, it would be imperative to perform an interval estimates to determine where the "true" speed (population mean) lies.

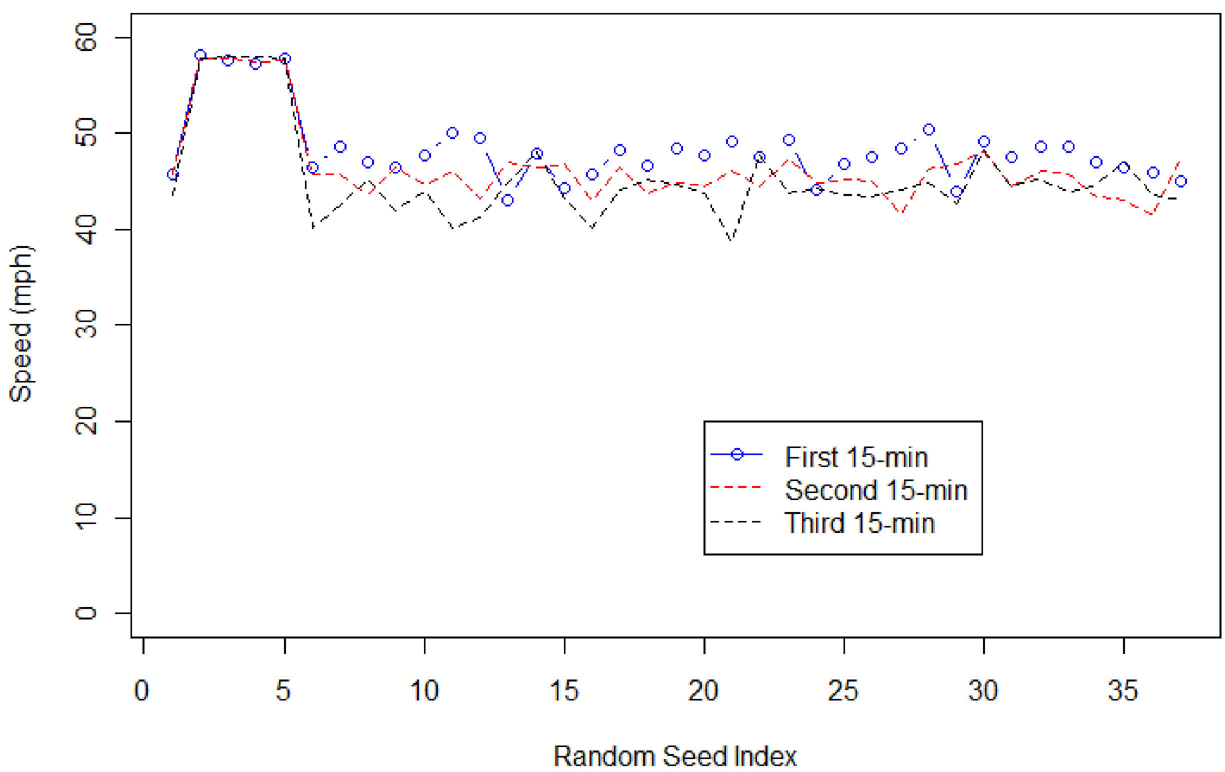

FIGURE 7.3 Speed profile for the Segment 1 GP Lane for three consecutive 15-min intervals under various random seeds.

Using the first 15-min data (shown in blue line in Figure 7.3), bootstrap statistics is performed. Figure 7.4 shows the histogram and quantile plots from the resampled data using the first 15-min data with a total of 37 random seed. The bootstrap can be considered as a resampling technique with permutation from the original sample. As the sampling size increases (in this case a total of 999 resamples are generated), the distribution of sample mean is approximately normal according to CLT, as shown in Figure 7.4 (a). With a total of 37 random seeds, the 95% CI through bootstrapping is determined to be (47.25, 49.51). That is, with 95% confidence, we can conclude that for the first 15-min, the average GP lane speed falls between 47.25 mph to 49.51 mph. In CI estimation, it is assumed that when the distribution for the population mean is unknown, and if the sample size is large enough, the traditional method is valid and applicable according to CLT. Normally, a sample size of 30+ would be considered large in common practice. With 37 samples, the 95% CI calculated through traditional method is (47.15, 49.55), which is quite close to the result generated from bootstrapping statistic method, only 5.83% wider. Following the same theoretical fashion, a sensitivity analysis is performed for both bootstrapping and traditional method under various numbers of random seeds (sample size), and the calculated 95% CI result is shown in Table 7.2. It is noted that as the number of samples increases, the standard error of the CI estimation is decreased. This effect is visualized in Figure 7.5 where the CI bounds are plotted in accordance with different numbers of random seeds. It is noted that the CI is more converged corresponding to a larger sample size. Although it is statistically incorrect to use the traditional method for the CI estimation with limited sample size (less than 30) and unknown population distribution, from the sensitivity analysis, it is observed that the traditional estimates did not generate significantly biased CIs, but only cover a wider range than the bootstrapping method. Therefore, for as long as computational resources allows, the bootstrapping statistics is recommended to conduct CI estimates in order to yield a better simulation estimation results.

From Table 7.2, note that with fewer random seeds, the standard error is higher. This is expected in that with limited sample size, the variation in estimating the true mean would be bigger which results in a higher probability of biased estimation. One way that is relatively easy to identify the optimal number of random seed would be to observe the resampling data's histogram using bootstrap. Figure 7.6 demonstrates the histogram of the resampled data with 5-8 random seeds. With more random seeds (larger sample size), the permutation would be performed more towards normal distribution. With eight random seeds as shown in Figure 7.6 (d), the histogram of the resampled data is already demonstrating the shape of a normal distribution. Therefore, a more convincing simulation result would be generated from eight random seed runs rather than five. That also shows the advantage of using bootstrap method in determining the optimal number of simulation runs which the traditional method would not be able to do.

Figure 7.7 shows the histogram from the original sample under different numbers of random seeds. No optimal random seed number could be identified from the histogram variations.

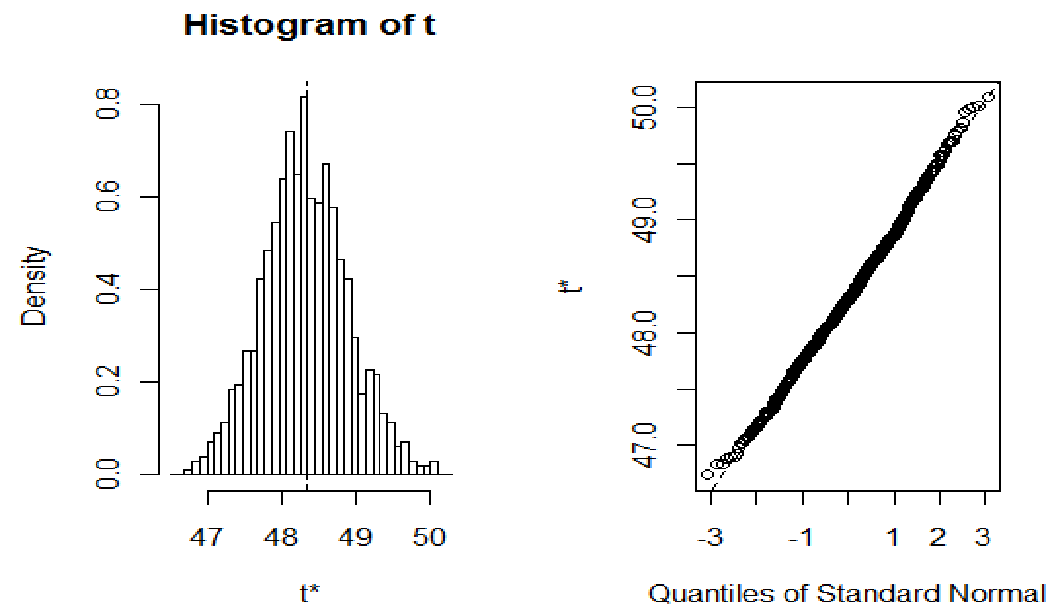

(a) Histogram of the Resample (b) Quantiles Plot

FIGURE 7.4 Histogram of the resampled data and quantiles plot from bootstrapping.

TABLE 7.2 95% confidence interval estimates under various numbers of random seeds.

Number of Random Seeds	Bootstrap			Traditional Estimates			CI Length Accuracy Improvement
	Standard Error	Lower CI	Upper CI	Standard Error	Lower CI	Upper CI	
5	2.14	51.10	59.52	2.40	50.57	59.98	10.52%
10	1.68	47.99	54.60	1.77	47.80	54.72	4.48%
15	1.25	47.40	52.28	1.35	47.17	52.46	7.75%
20	1.01	47.19	51.15	1.04	47.16	51.23	2.70%
25	0.81	47.20	50.41	0.86	47.14	50.51	4.75%
30	0.722	47.28	50.11	0.735	47.22	50.11	2.08%
35	0.647	47.28	49.82	0.634	47.27	49.76	-2.01%
37	0.576	47.25	49.51	0.611	47.15	49.55	5.83%

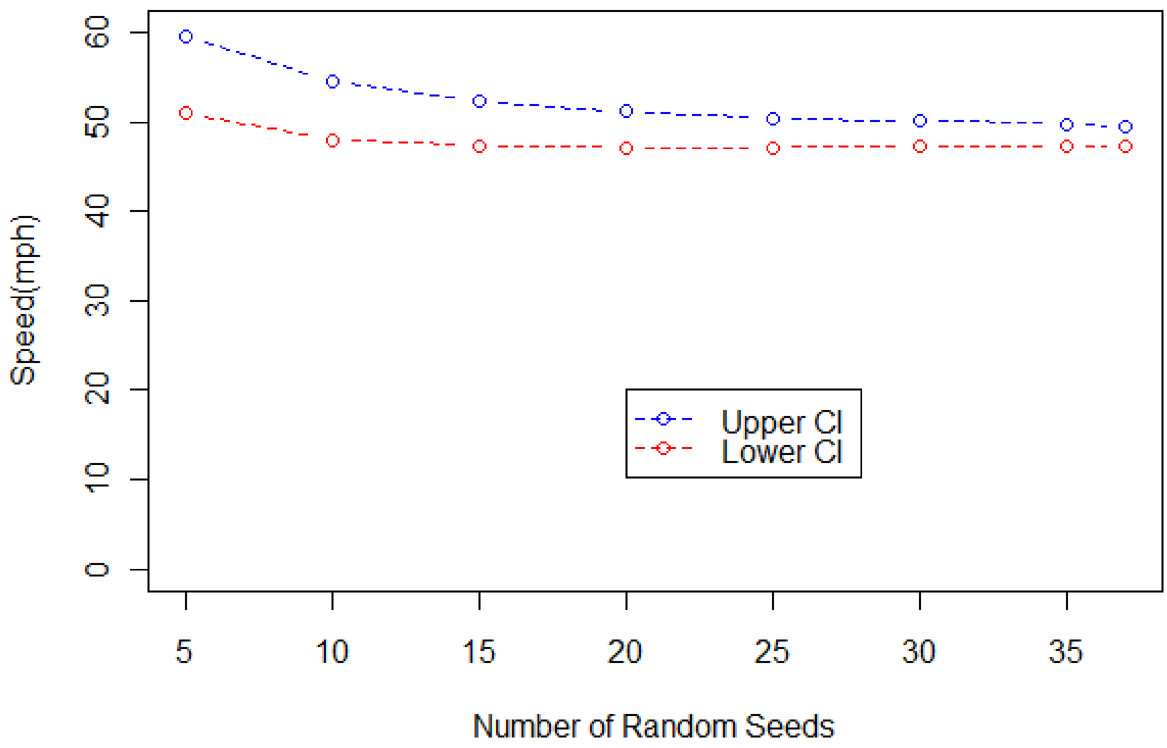

FIGURE 7.5 95% CI bounds under various numbers of random seeds using bootstrap.

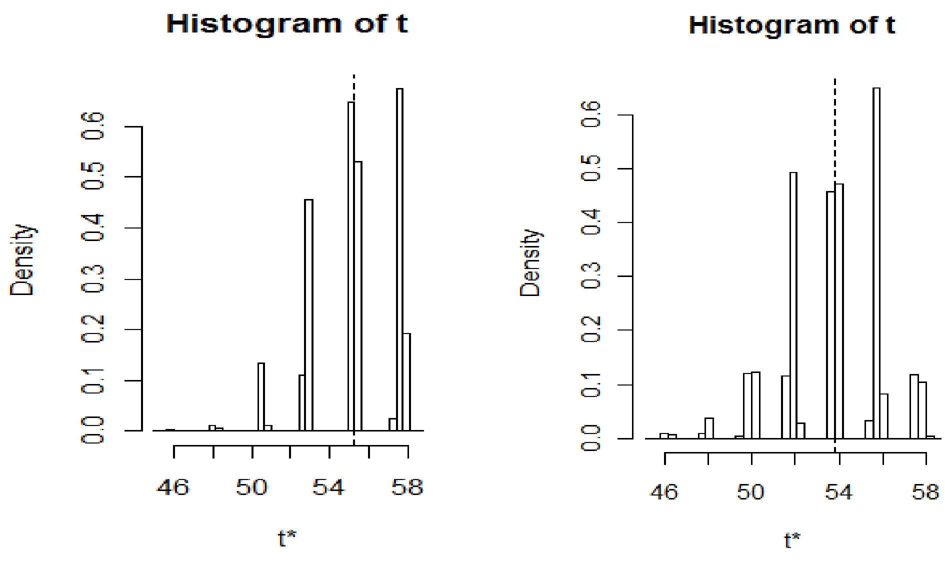

(a) Five Random Seeds

(b) Six Random Seeds

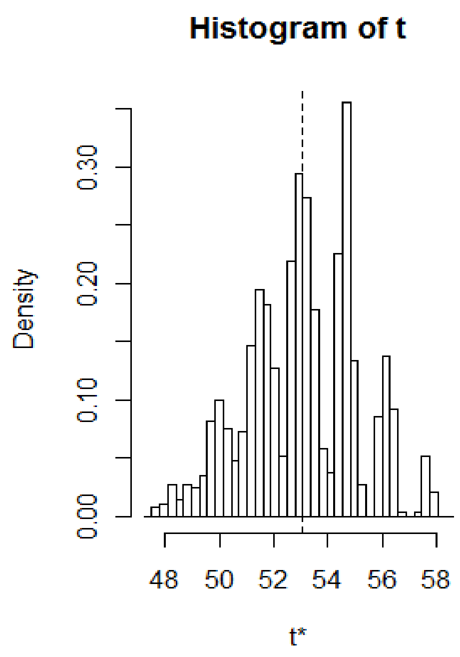

(c) Seven Random Seeds

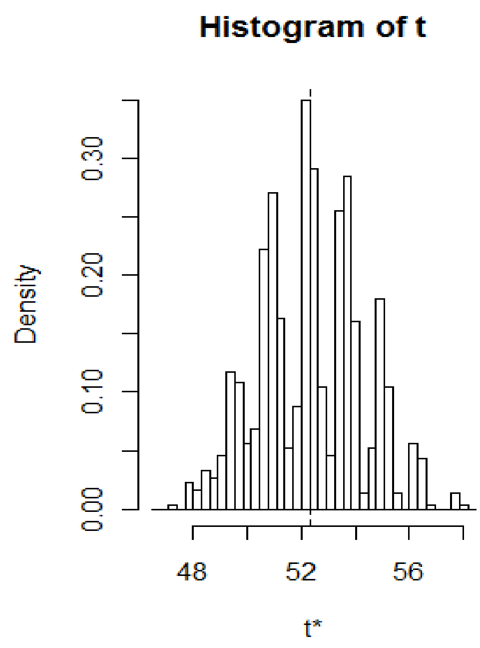

(d) Eight Random Seeds

FIGURE 7.6 Histogram of the resampled data under various numbers of random seeds.

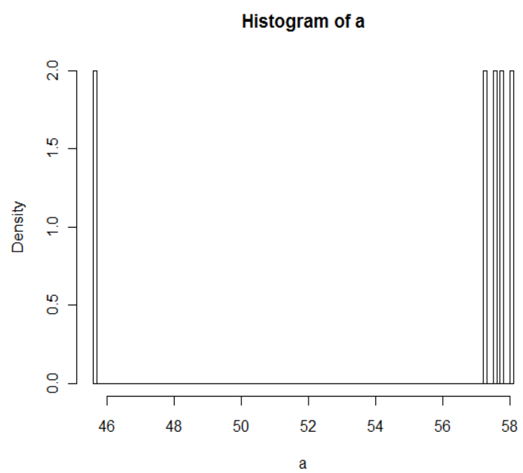

(a) Five Random Seeds

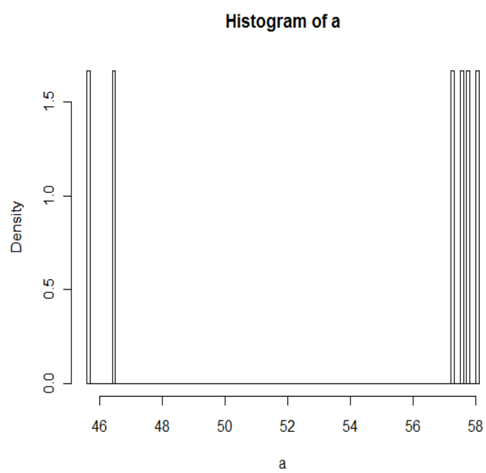

(b) Six Random Seeds

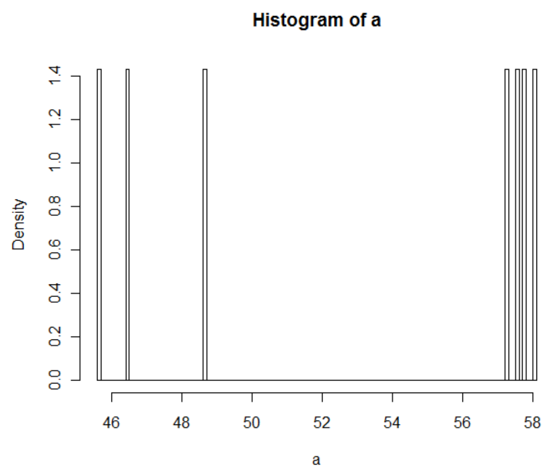

(c) Seven Random Seeds

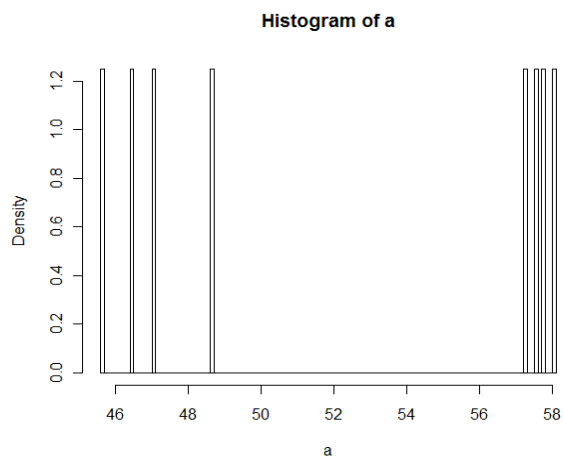

(d) Eight Random Seeds

FIGURE 7.7 Histogram of the original sample under various numbers of random seeds.

7.2.2 Interval Estimates from Single Simulation Run

To construct the CI from a single simulation run, it is necessary to investigate the autocorrelation function (ACF) from the data. The GP lane speed at Segment 1 is again chosen to demonstrate the analysis procedure. The simulation run with Random Seed Index of 193 is performed, and second-by-second speed data were collected. To eliminate the initial transient state of the simulation, data from 900 to 9,900 simulation seconds were extracted. To compare the CIs constructed from various simulation resolutions, the data are further aggregated into 1-minute, 5-minute and 15-minute. The ACF is defined in Equation 7.1. Figure 7.8 shows the ACFs for the GP lane speed data aggregated at different resolutions. The ACF for the second-by-second output shows that the speed data are highly correlated. As the data were aggregated at higher intervals, the correlation effect is weakened. For 1-minute aggregation, after Lag 4, the correlation coefficients are considered insignificant at 95% confidence interval. For the 5-minute aggregation, after Lag 1, the correlation coefficients are considered insignificant at 95% confidence interval. It also demonstrates that, as the aggregation level increases, the simulation output can be modeled using certain typical time series models such as First-Order Autoregressive Process (AR(1)), as the data appear to be in a stationary process.

$$\rho_x(h) = \frac{\gamma_x(h)}{\gamma_x(0)} = \frac{cov\{X_{t+h}, X_t\}}{\sqrt{var\{X_{t+h}\}var\{X_t\}}} \tag{7.1}$$

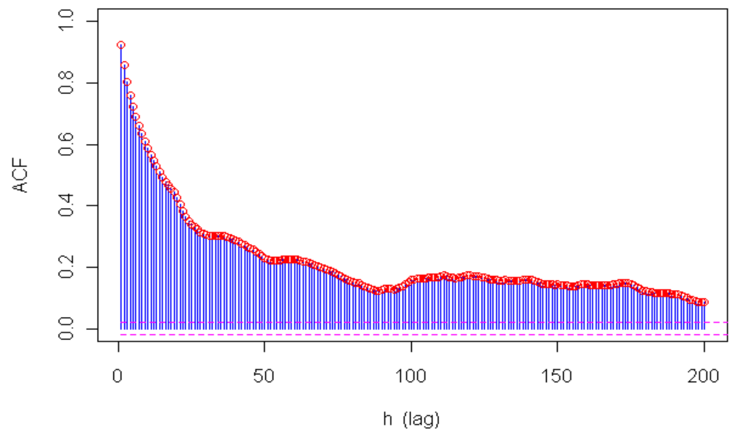

(a) Aggregated at 1-second Time Interval

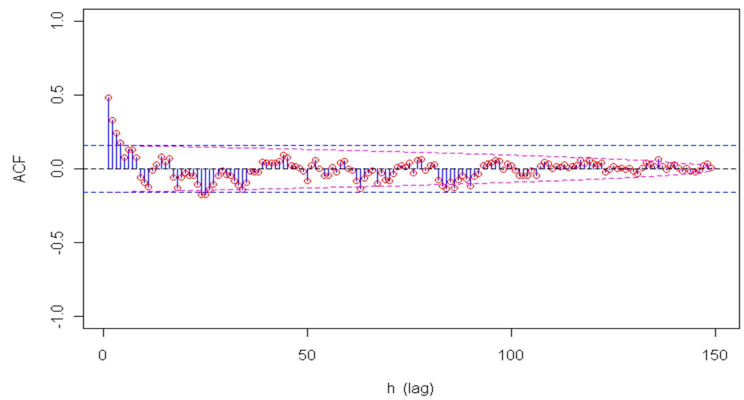

(b) Aggregated at 1-min Time Interval

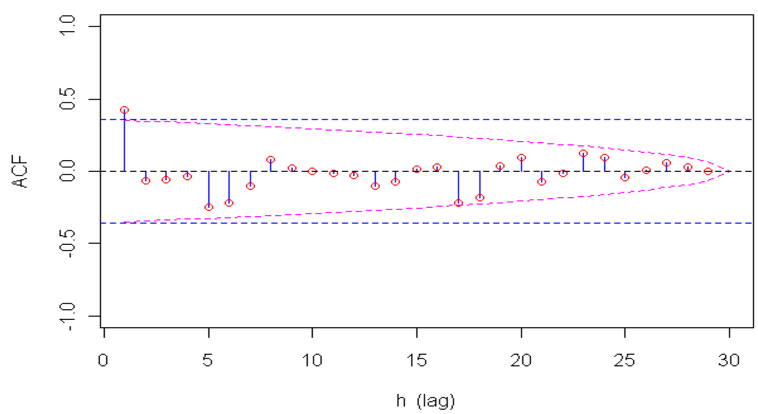

(c) Aggregated at 5-min Time Interval

FIGURE 7.8 ACF for the GP lane speed data aggregated at 1-second, 1-minute, and 5-minute, separately.

Considering the autocorrelation problem, the method proposed in Chapter 4 is used to calculate the sample variance. Using second-by-second data, $Var(\bar{S}_M) = 0.111282$. The data are further aggregated by different time intervals, including 1-minute, 5-minute and 15-minute. The calculated $Var(\bar{S}_M)$ are 0.3762199, 0.7310445, 1.017054, separately. The CI constructed from different aggregation resolutions are shown in Table 7.3. Also in Table 7.3, the CI constructed using the traditional method is demonstrated. The proposed method is more reasonable in that the higher the aggregation level, the more dispersed the data would be. Thus, correspondingly, the standard error would be higher from sample estimates. The last column in Table 7.3 shows the stand error difference between the two methods using the proposed method as a reference. It is noted that, for most of the cases (1-second, 5-minute, and 15-minute), the traditional method tends to be over optimistic about the CI estimation. As the aggregation level increases, the standard error difference is less significant. This can be traced back to the autocorrelation problem discussed. As shown earlier in Figure 7.8, as the aggregation level increases, the autocorrelation effect is weakened. Correspondingly, the bias in using the two different methods for interval estimates is less.

TABLE 7.3 CI constructed from different aggregation levels.

Aggregation Level	Proposed Method			Traditional Estimates			Standard Error Difference
	Standard Error	Lower CI	Upper CI	Standard Error	Lower CI	Upper CI	
1-second	0.33	43.12	44.42	0.07	43.64	43.91	78.8%
1-minute	0.62	42.57	44.98	1.44	40.95	46.60	-132%
5-minute	0.85	42.10	45.45	0.58	42.65	44.90	32.3%
15-minute	1.01	41.79	45.76	0.73	42.35	45.20	27.7%

CHAPTER 8 CONCLUSIONS AND RECOMMENDATIONS

8.1 Conclusions

This research chooses two toll roads, SR-167 HOT Lanes and SR-520 Bridge, as study sites for testbed developments for evaluating how tolling strategies affect freeway operations. For the SR-167 HOT Lane testbed, three manage strategies and three traffic demand conditions are considered and compared in this research. The simulation results found that among all the three operational strategies, HOT Lane Operation with Dynamic Toll outperformance the other two strategies under various traffic demand condition. Compared with the HOV Lane Operation, Dynamic Toll strategy makes significant improvement on GP lane performance, merging areas, on-ramps, and off-ramps are significant. Compared with the Time-of-day Toll Rate strategy, Dynamic Toll strategy is more flexible under a variety of traffic demand.

For the SR-520 toll bridge simulation, two scenarios were considered. In scenario 1, the traffic demand is assumed to be the same before and after the toll implementation. Four different tolling rates are considered in this scenario: \$0, \$1, \$3.5, \$7. In scenario 2, it is assumed that there is a 5% reduction in traffic demand on SR 520 during peak hour. The simulation results of the SR-520 Bridge found that with an increase in toll at SR-520, the travel speed on SR-520 tends to increase and the speed on I-90 tends to decrease as more vehicles are diverted to use the non-tolled alternative. The overall trend of speed and volume under scenario 2 is similar with the results from dual data.

In the simulation model development, an appropriate approach to analyze the simulation output is of outmost importance. It not only affects the fidelity and credibility of the model, but also has an influence on the cost and time spent on the simulation project. One of the key issues for the output analysis is to determine the confidence interval of different output MOEs. In all simulation software packages, including VISSIM, simulation models utilize the pseudo-random number sequence (random seed) to emulate the randomness in reality. The variations in different random seeds would affect the realization of the stochastic quantities in VISSIM, such as inlet flows and vehicle capabilities. The data sets from different random seeds are considered IID time series. To determine the accurate confidence interval from limited simulation runs, a computer simulation technique called “bootstrap” is applied in this research. Bootstrap is a model-free based resampling approach that can populate simulation data from the original data set through permutation. Sensitivity analysis from different number of simulation runs were conducted for both bootstrapping method and conventional statistical method for interval estimation. It is determined that bootstrapping approach can more accurately estimate the confidence interval than the conventional approach.

Besides the interval estimates from multiple simulation runs, it is also imperative to perform similar estimates for the MOEs from a single simulation run. However, the output data from a single run are auto-correlated, which does not meet the requirement for IID to construct confidence interval using the conventional method. Therefore, a new statistical approach is developed to take into account the auto-correlation effect for interval estimation. Confidence interval constructed at different aggregation level was investigated to compare the proposed method with the conventional one. It is also determined that the proposed method can more accurately reflect and auto-correlation effect at various aggregation level.

8.2 Recommendations

On the basis of the findings of this study, the research team would like to make the following recommendations:

- Use dynamic tolling strategy when possible since it is more flexible to respond to the real-time traffic conditions than other tolling strategies.
- More research is desired for improving the accessibility from I-450 to I-90 and from SR-520 WB to I-405 SB when SR-520 is tolled.
- More research is needed for developing traffic responsive dynamic tolling strategies.

REFERENCES

1. Alexopoulos, C. (2006). A Comprehensive review of methods for simulation output analysis. In Proceed-ings of the 2006 Winter Simulation Conference, 168-178. Piscataway, New Jerse.
2. Appiah J., M. W. Burris, (2005) QuickRide User Response to Different HOT Lane Operating Scenarios, In the 84th annual meeting of the Transportation Research Board, CD-ROM. Transportation Research Board, National Research Council, January, Washington, D.C., 2005
3. Banks, J., J. S. Carson, B. L. Nelson, and D. M. Nicol. (2005). Discrete-event system simulation, 4th ed. Up-per Saddle River, New Jersey: Prentice-Hall.
4. Bureau of Transportation Statistics. (2010). “National Transportation Statistics 2010”. U.S. Department of Transportation. Washington, D.C.
5. CBO MEMORANDUM,(1997). Toll Roads: a Review of Recent Experience. Congressional Budget Office, Washington, DC.
6. Chew, V., (2008). Electronic Road Pricing: Developments After Phase I. National Library Singapore, Singapore Infopedia http://infopedia.nl.sg.offcampus.lib.washington.edu/articles/SIP_1386_2009-01-05.html (25.07.09).
7. Cambridge Systematics, Inc.(2007). PSRC 2006 Household Activity Survey Analysis Report. Final report.
8. Chu, L, K. S. Nesamani, and H. Benouar (2007) Priority Based High Occupancy Vehicle Lanes Operation, In the 86th annual meeting of the Transportation Research Board, CD-ROM. Transportation Research Board, National Research Council, January 22-26, Washington, D.C., 2007.
9. Craig J. Stone, Dave Dye, Paula Hammond, Steve Reinmuth, (2012) WSDOT Toll Division Update. Washington State Transportation Commission Olympia, WA, February 21, 2012.
10. Dahlgren D., (1998) High Occupancy Vehicle Lanes: Not Always More Effective Than General Purpose Lanes. Transportation Research A, Vol. 32. No. 2 pp. 99-114.
11. De Palma, A., Kilani, M., Lindsey, R., (2005). Congestion pricing on a road network: a study using the dynamic equilibrium simulator METROPOLIS. Transportation Research A Vol. 39 No. 7, 588–611.
12. De Palma, A; Lindsey, R. (2011). Traffic congestion pricing methodologies and technologies, Transportation Research C, Volume 19, Issue 6, pp. 1377-1399.
13. DeCorla-Souza, P., and Kane, A. (1992). Pick period tolls: Precepts and prospects. Transportation Vol. 19, 293-311.
14. Encyclopedia Britannica, (2005). Encyclopedia Britannica 2005 Deluxe Edition.

15. Gomes G. A. May and R. Horowitz. (2004) Congested Freeway Microsimulation Model Using VISSIM. In Transportation Research Record: Journal of Transportation Research Board, No.1876, TRB, National Research Council, Washington, D.C., , pp. 71-81.
16. Hall, R.W., (1986). The Fastest Path through a Network with Random Time-Dependent Travel Times. Transportation Science, 20(3), pp.182-188.
17. Halvorson, R., M. Nookala, and K. R. Buckeye, (2006). High occupancy toll lane innovations: I-394 MnPASS. In the 85th annual meeting of the Transportation Research Board, CD-ROM. Transportation Research Board, National Research Council, January 22-26, Washington, D.C., 2006.
18. Jose Holguin-Veras, Mecit Cetin, Shuwen Xia, (2006). A comparative analysis of US toll policy, Transportation Research Part A Vol. 40 No. 10. 210-218
19. Kalmanje, S., and Kockelman, K. (2005). Toll roads in Texas: Traffic and welfare impact. Accessed on Feb 18, 2008, from http://www.ce.utexas.edu/prof/kockelman/public_html/ TRB06SukumarTRs.pdf.
20. Kim, A.M., Y. Gardes, and A.D. May (2002), Application Of The Paramics Model In High Occupancy Vehicle Lane Operations. 9th World Congress on Intelligent Transport Systems. Chicago.
21. Kockelman, K.M., Kalmanje, S., (2005). Credit-based congestion pricing: a policy proposal and the public's response. Transportation Research A Vol. 39 No. 9, 671–690.
22. Kwon, J. and Varaiya, P. (2005). Effectiveness of High Occupancy Vehicle Lanes in San Francisco Bay Area. University of California, Berkeley and California State University, East Bay, California.
23. Law, A. M. (2007). Simulation modeling and analysis, 4th ed. New York: McGraw-Hill.
24. Lelewski, A R; Berenis, J A; Pressimone, G M. (2003) Analyzing Express Toll Plaza Operations Using Modern Simulation Models Institute of Transportation Engineers 2003 Annual Meeting.
25. Ma, X., Wu Y., Wang. Y., (2011). DRIVE Net: An E-Science of Transportation Platform for Data Sharing, Visualization, Modeling, and Analysis. Transportation Research Record: Journal of the Transportation Research Board. No. 2215. 2011. pp 37-49.
26. Marlon, B., and Chalermpong, S. (2001). New highways, house prices and urban development: A case study of toll roads in Orange county, CA. Housing policy Debate Vol.12, No. 3, 575-605.
27. Mowday, M. (2006) Equity and High Occupancy Toll Lanes: A Literature Review and Minnesotans Perceptions About the I-394 High Occupancy Toll Lanes. In the 85th annual meeting of the Transportation Research Board, CD-ROM. Transportation Research Board, National Research Council, January 22-26, Washington, D.C., 2006.
28. Myron S., and D. Ungemah, (2006) So You Want To Make a Hot Lane? The Project Manager's Guide For an Hov-To-Hot Lane Conversion. In the 85th annual meeting of the Transportation

Research Board, CD-ROM. Transportation Research Board, National Research Council, January, Washington, D.C., 2006.

29. Papageorgiou, M., H. Haj-Salem, and F. Middelham, (1997) ALINEA local ramp metering: summary of field results. In Transportation Research Record: Journal of Transportation Research Board, No. 1603, TRB, National Research Council, Washington, D.C.,1997, pp. 90-98.
30. Parasibu, M. (2005). The role of toll roads in promoting regional development: Private sector participation: A case study of Jabotabek. Accessed Feb, 28, 2008, from http://www.sustainabledevelopment.org/learning/casebooks/uncrd/parasibu.pdf.
31. Pigou, A.C., (1920). The Economics of Welfare. Macmillan and Co., London.
32. PTV. (2007). "Vissim User Manual - V.4.30”. Karlsruhe, Germany.
33. PTV. (2010). VISSIM 5.30-01 - Car2X Interface Manual. Karlsruhe, Germany.
34. PTV. (2011). Vissim 5.30-04 User Manual. Karlsruhe, Germany.
35. Puget Sound Freeway and HOV Performance Statistics. (2008). http://depts.washington.edu/hov/. Accessed 2008.
36. Ruppert, D. (2011). Statistics and Data Analysis for Financial Engineering. 1st Edition. Springer.
37. Schrank, D., Lomax, T., (2009). The 2009 Urban Mobility Report. College Station: Texas Transportation Institute, Texas A&M University. http://mobility.tamu.edu.offcampus.lib.washington.edu (16.07.09).
38. ShrunkShrank, D. and T. Lomax. (2011) The 2011 Urban Mobility Report. Texas Transportation Institute. The Texas A&M University System (http://mobility.tamu.edu/).
39. Verhoef, E.T., (2002). Second-best congestion pricing in general static transportation networks with elastic demands. Regional Science and Urban Economics Vol. 32, No. 9. 281–310.
40. Verhoef, E.T., (2005). Speed-flow relations and cost functions for congested traffic: theory and empirical analysis. Transportation Research A. Vol. 39 No. 7, 792–812.
41. Welch, P. D. (1983). The statistical analysis of simulation results. The Computer Performance Modeling Handbook, ed. S. S. Lavenberg. New York: Aca-demic Press.
42. Wiedemann. R. (1991). “Modeling of RTI-Elements on multi-lane roads.” Advanced Telematics in Road Transport, Vol. DG XIII.
43. WSDOT, (2011). http://www.wsdot.wa.gov/Tolling/TollRates.htm. (05.11.11).
44. WSDOT. (2010). Peak hour report 2010. Statewide Travel Collision Data Office.
45. Yan, H., Lam, W.H.K., (1996). Optimal road tolls under conditions of queuing and congestion. Transportation Research A Vol. 30 No. 5, 319–332.

46. Yin, Y., and Y. Lou. (2007). Dynamic Tolling Strategies for Managed Lanes. In the 86th annual meeting of the Transportation Research Board, CD-ROM. Transportation Research Board, National Research Council, January 21-25, Washington, D.C., 2007.
47. Zhang, G, Wang Y., Wei H. and Yi P., (2008) A Feedback-Based Dynamic Tolling Algorithm for High Occupancy Toll (HOT) Lane Operations, Transportation Research Record: Journal of the Transportation Research Board, No. 2056. pp 54-63.
48. Zhang, G., Yan, S., and Wang. Y., (2009) Simulation-based Investigation on High Occupancy Toll (HOT) Lane Operations for Washington State Route 167. ASCE Journal of Transportation Engineering. Vol. 135, No. 10, 2009. pp 677-686.
49. Zhang, H.M., Ge, Y.E., (2004). Modeling variable demand equilibrium under second-best road pricing. Transportation Research B Vol. 38 No. 8, 733–749.
50. Zmud J., S. Peterson, F. Douma. (2007) Preliminary Before and After Results of the I-394 HOT Lane Panel Survey. In the 86th annual meeting of the Transportation Research Board, CD-ROM. Transportation Research Board, National Research Council, January 21-25, Washington, D.C., 2007.
51. Zmud. J., M. Bradley, F. Douma, and C. Simek, (2007) Panel Survey Evaluation of Attitudes and Willingness to Pay for Tolled Facilities. In the 86th annual meeting of the Transportation Research Board, CD-ROM. Transportation Research Board, National Research Council, January, Washington, D.C., 2007.

APPENDIX

Simulation Output Analysis: R Code

```
library(PerformanceAnalytics)
library(zoo)
library(mvtnorm)
library(boot)
library(tseries)
RS=read.csv("C://Users/CathyAdmin/Desktop/CongestionPricing/AVGRS.csv"
,header=TRUE,sep=",")
plot(RS[1,],xlab="Random Seed Index",ylab="Speed
(mph)",typ="b",col="blue",ylim=c(0,60),pch=1,lty=1)
lines(RS[2,],xlab="Random Seed Index",ylab="Speed
(mph)",pch=16,col="red",ylim=c(0,60),lty="dashed")
lines(RS[3,],xlab="Random Seed Index",ylab="Speed
(mph)",pch=4,col="black",ylim=c(0,60),lty="dashed",legend.text=lbls)
legend(list(x=20,y=20),c("First 15-min","Second 15-min","Third 15-
min"),col=c("blue","red","black"),lty=c(1,2,2),pch=c(1,n,n)

tt=as.matrix(RS)
a=tt[1,1:35]
n=35
mean(a)+1.96*sd(a)/(n)^0.5
mean(a)-1.96*sd(a)/(n)^0.5
sd(a)/(n)^0.5
x.mean.boot = boot(a, statistic = mean.boot, R=999)
x.mean.boot
boot.ci(x.mean.boot, conf = 0.95, type = c("norm","perc"))
plot(x.mean.boot)
t=as.matrix(x)[,1]
n=length(t)
ts.acvf <- acf(t, lag.max=n, type="covariance", plot=TRUE)
sum=0
for (i in 1:n)
    {
  sum=sum+2*(1-i/n)*ts.acvf$acf[i]
}
vartheta=(1/n)*(ts.acvf$acf[1]+sum)
y=t
n=length(y)
k=seq(from=1,to=n,by=1)
a.n=1-k/n
var.y=var(y)
sd.y=sd(y)
cov=ts.acvf$acf
y.mean.var=1/n*(var.y+2*t(a.n)%*%cov)


CI=read.csv("C://Users/CathyAdmin/Desktop/SimulationTestBed/CI.csv",he
ader=TRUE,sep=",")
```

```
 a=CI[,1]
b=CI[,3]
c=CI[,4]
plot(a,b,xlab="Number of Random
Seeds",ylab="Speed(mph)",ylim=c(0,60),col="red",lty="dashed",typ="b")
lines(a,c,lty="dashed",typ="b",col="blue")
legend(list(x=20,y=20),c("Upper CI","Lower
CI"),col=c("blue","red"),lty=c(2,2),pch=c(1,1))
ts.sec <-
scan("C://Users/CathyAdmin/Desktop/SimulationTestBed/1sec.txt")
ts.sec <-
scan("C://Users/CathyAdmin/Desktop/SimulationTestBed/1min.txt")
ts.sec <-
scan("C://Users/CathyAdmin/Desktop/SimulationTestBed/5min.txt")
ts.sec <-
scan("C://Users/CathyAdmin/Desktop/SimulationTestBed/15min.txt")
#plot the ACF for the second-by-second time series
n.lags <- length(ts.sec)
n<-length(ts.sec)
ts.r.acf <- acf(ts.sec, lag.max=n.lags, plot=FALSE)
n <- length(ts.sec)
CI.hw <- 1.96/sqrt(n)
xs <- 1:n.lags
ys <- ts.r.acf$acf[2:(n.lags+1)]
plot(xs,ys,typ="h",xlab="h  (lag)",ylab="ACF",ylim=c(-1,1),col="blue")
points(xs,ys,col="red")
xs <- 1:(n.lags+1)
lines(xs,1.96*sqrt(n-xs)/n,col="magenta",lty="dashed")
lines(xs,-1.96*sqrt(n-xs)/n,col="magenta",lty="dashed")
abline(h=0,lty="dashed")
abline(h=c(-CI.hw,CI.hw),col="blue",lty="dashed")
phi <- ts.r.acf$acf[2]
round(phi,3)
lines(xs,phi^xs)
```